MODELING THE INTERACTION OF *MYCOPLASMA PNEUMONIAE* WITH GLYCAN RECEPTORS

by

CAITLIN REEVES WILLIAMS

(Under the Direction of Duncan C. Krause)

ABSTRACT

Mycoplasma pneumoniae is a common cause of human respiratory tract infections and best known as the etiologic agent of atypical or "walking" pneumonia. *M. pneumoniae* binds to glycoprotein receptors having terminal sialic acid residues and glycolipids having sulfate functional groups. In this dissertation, we utilized two *in vitro* models to explore the impact of terminal sialic acid and sulfate presentation on *M. pneumoniae* adherence and gliding. We utilized surfaces coated with the sialylated glycoproteins laminin or human chorionic gonadotropin (hCG) or the sulfated glycolipid sulfatide; and chemically functionalized surfaces having α-2,3- and α-2,6-sialyllactose ligated individually or in combination to a polymer scaffold in precisely controlled densities. Both sialylated and sulfated receptors supported *M. pneumoniae* adherence, but gliding motility was only present on laminin and α-2,3-sialyllactose. The density of sialylated residues influenced *M. pneumoniae* gliding frequency but not gliding speed, and gliding required a receptor density threshold higher than that needed to support adherence. However, at very high α-2,3-sialyllactose densities gliding frequency was actually reduced relative to peak gliding noted at lower receptor densities. Finally, gliding on α-2,3-sialyllactose was inhibited on surfaces also conjugated with α-2,6-sialyllactose. Thus, both α-2,3- and α-2,6-

sialyllactose may bind P1 adhesin complexes despite the inability of the latter to support gliding. Terminal organelle mutants were also utilized to further elucidate the interaction of *M. pneumoniae* adhesins and sialylated and sulfated receptors. The absence of functional terminal organelle protein P30, which results in non-functional P1, resulted in loss of attachment to sialylated but not sulfated receptors. Indicating that sulfated receptors may interact with an alternate adhesin than the P1 complex. In summary, the nature and density of host receptor moieties can have a profound influence on *M. pneumoniae* gliding, which could in turn affect pathogenesis, persistence, and infection outcome.

INDEX WORDS: *Mycoplasma pneumoniae*, Glycan Receptors, Gliding Motility

MODELING THE INTERACTION OF *MYCOPLASMA PNEUMONIAE* WITH GLYCAN RECEPTORS

by

CAITLIN REEVES WILLIAMS

B.S., Virginia Tech, 2012

A Dissertation Submitted to the Graduate Faculty of The University of Georgia in Partial Fulfillment of the Requirements for the Degree

DOCTOR OF PHILOSOPHY

ATHENS, GEORGIA

2018

© 2018

Caitlin Reeves Williams

All Rights Reserved

MODELING THE INTEARCTION OF *MYCOPLASMA PNEUMONIAE* WITH GLYCAN RECEPTORS

by

CAITLIN REEVES WILLIAMS

Major Professor:	Duncan C. Krause
Committee:	Robert J. Maier
	Vincent Starai
	Michael Tiemeyer

Electronic Version Approved:

Suzanne Barbour
Dean of the Graduate School
The University of Georgia
May 2018

DEDICATION

This work is dedicated to two of the most influential people in my life. For Colin, my loving husband, who has been there throughout the past six years from boyfriend to husband. He has been there to celebrate my triumphs, but more importantly help me through the rough patches. Your unwavering support made this degree possible. Thank you for always reminding me of my strength and believing in me.

And for my mother, Linda Reeves, who has never stopped believing in me. You have been there from day one to celebrate my success and help me through my failures. You have always encouraged me to chase my dreams and been by my side to support me in every way. I would not be where I am today without you. Thank you for showing me what it means to be a strong, intelligent, and caring woman. I am forever thankful for your love and all that you do for me.

ACKNOWLEDGEMENTS

I am incredibly grateful and thankful for my doctoral advisor Dr. Duncan C. Krause. I am fortunate to have worked as a student in his lab and know I will never find another mentor quite like him. I am appreciative of his guidance in both science and life throughout these past six years. Thank you for pushing me to grow as a person and scientist and always being supportive.

I would like to thank Ed Sheppard for all his help in the lab from teaching me everything I know about working with mycoplasma and spending countless hours helping me troubleshoot and run experiments. Learning from you, working alongside of you, and getting to know you has been a great joy. I would also like to the thank all of the Krause lab members who came before me for their guidance, support, and creation of an amazing lab environment. I would like to thank Dr. Jason Locklin and his graduate students Dr. Rachelle Arnold, Deb Leman, and Li Chen for the work and help they put in on the functionalized surface project.

I am grateful to have come in to graduate school with a wonderful cohort, thank you for making these past years bearable and memorable. Kara Tinker, for always being there for me and becoming one of the best friends I could ever ask for. I am also appreciative to all the friends I have made inside and outside the department, thank you for helping to make this experience even more memorable.

TABLE OF CONTENTS

Page

LIST OF TABLES

Page

LIST OF FIGURES

Page

CHAPTER 1

INTRODUCTION

Mycoplasma pneumoniae, best known as the etiologic agent of "walking pneumonia", is a common cause of respiratory tract infections. It is responsible for as many as 40% of community-acquired pneumonias (CAP) in both adults and children (1). Due to a lack of effective tools for diagnosis it is a common misperception that incidence of infection is rare (2). Infections can manifest in the upper and lower respiratory tract of humans. *M.* pneumoniae has also been linked to some chronic human diseases such as asthma and chronic obstructive pulmonary disease (COPD), in which the organism persists and is difficult to clear from the body (2, 12, 13). However, the molecular basis for this persistence is unknown, severely limiting our ability to reduce incidence and impact of disease caused by *M. pneumoniae*.

Both attachment (3-8) and gliding motility (9-11) are essential for effective colonization. *M. pneumoniae* is known to recognize two distinct receptor populations: α 2-3 linked sialic acid (SA)-containing sialoglycoproteins (SGP) and sulfated glycolipids (SGL) such as sulfatide (14, 15). When the terminal sialic acid of these sialoglycoproteins is cleaved by neuraminidase treatment, adhesion activity is lost (16). Another study showed that free sialylated compounds inhibited binding of *M. pneumoniae* to glass, and removed gliding mycoplasma attached to a surface (17). For glycolipids, mycoplasma binding specificity was shown only for sulfated glycolipids with Gal(3SO_4)β1 residues, with the presence of dextran sulfate, a sulfatide binding inhibitor,

leading to decreased attachment (14). These findings led to the idea that differences in receptor environment may be fundamentally important to the outcome of airway colonization. However, binding of mycoplasma to these glycan moieties has not been studied in depth, and understanding of the human airway glycome is limited. Elucidating the interactions between *M. pneumoniae* and receptor moieties could lead to a better understanding of mycoplasma-host interaction.

The purpose of this dissertation is to further elucidate the interaction of *M. pneumoniae* binding to SGP and SGL and the impact of relative abundance of each on gliding activity. The more traditional approach of chamber slides coated with sialoglycoproteins and sulfated glycopids at varying concentrations will be utilized. However, the use of full proteins has limitations due to size and variation in sialylation, so a new model system was developed. Glass surfaces were chemically functionalized with sialylated sugars to allow for a more precise and controlled approach. Sugars were conjugated at varying concentrations, as well as functionalizing varying ratios of different sialyloligosaccharides.

There were 3 objectives:

Aim 1: Define the gliding phenotype of *M. pneumoniae* on sulfated and sialylated receptors.

Aim 2: Determine the role that sulfated and sialylated receptor concentration plays in *M. pneumoniae* attachment and gliding.

Aim 3: Determine the role of the P30 protein in attachment and gliding motility on sulfated and sialylated receptors.

CHAPTER 2

REVIEW OF THE LITERATURE

Mycoplasma Overview

Taxonomic class Mollicutes – "Soft Skin". Within the phylum *Tenericutes* the genus *Mycoplasma* contains 200 established species that live in a wide variety of hosts as both commensals and pathogens (18). Host species are widespread, from humans and mammals to reptiles, arthropods, and plants (19). *Mycoplasma* species dwell in a large number of vertebrates, both wild and domesticated, including livestock and household pets. Pigs are home to the commensal organism *M.hyorhinis,* as well as the pathogen *M. hyopneumoniae,* while cows play host to the pathogens *M. bovis* and *M. mycoides*, and poultry to *M. gallisepticum* and *M. synoviae*. Mycoplasmas also infect our household pets. such as cats (*M. haemofelis*) and dogs (*M. canis* and *M. arginini*). In the wild. there are mycoplasmas found in tortoises (*M. agassizii*), fish (*M. mobile*), and alligators (*M. alligatoris*). The human mycoplasmas include commensals such as *M. orale* and *M. salivarium,* as well as the respiratory pathogen *M. pneumoniae* and the sexually transmitted species *M. genitalium* and *M. penetrans*. Mycoplasma have been found to infect a wide range of hosts in a variety of environments.

The mycoplasmas are characterized by small genomes diverged from the *Streptococcus* branch of gram-positive bacteria 605 million years ago (20). These minimal genomes range from 580 kb to over 2000 kb, with the UGA codon used for tryptophan instead of a stop codon (9, 18, 19). Mycoplasma species are unique within

their Domain due to their lack of peptidoglycan cell walls typically found in most bacterial species (19). These bacteria have a plasma membrane and underlying cytoskeleton that helps to maintain cell shape and plays a role in cell division. The plasma membrane is fairly typical, and by mass is over 2/3 protein, with the rest of the membrane mass consisting of lipids (21). Fatty acid residues of phosopholipids, glycolipids, and cholesterol constitute a major portion of the hydrophobic core of the membrane (18). The mycoplasmas are predominantly pleomorphic, with some being pear- or flask- shaped with terminal structures (18).

The small range of genome size in the mycoplasmas has led to a limitation in metabolic capabilities. Mycoplasmas grow as aerobes or facultative anaerobes and have truncated respiratory systems. No oxidative phosphorylation is possible due to the lack of quinones and cytochromes and an incomplete tricarboxylic acid cycle (22). This leads to low ATP yields, requiring the bacteria to obtain metabolic end-products from host tissues (23). Many mycoplasma species encode the enzymes necessary for arginine catabolism, including arginine deiminase, ornithine carbamoyltransferease and carbamate kinase. This allows for arginine to be acquired from the host and degraded to produce ATP (24). Some species, including *M. pneumoniae* and *M. genitalium*, carry enzymes for the Embden-Meyerhof-Parnas pathway to metabolize glucose (18).

A majority of mycoplasma species also require lipids and lipid precursors for synthesis of the membrane, but no genes involved in synthesis of fatty acids or cholesterol are present (25). Acquisition of these lipids from the host or the addition of cholesterol to growth medium is necessary for mycoplasma growth (26-28). *M. pneumoniae* genome analysis has revealed a lack of nucleoside diphosphate kinase, the

essential enzyme for conversion of nucleoside diphosphate to nucleoside triphosphate (25). The protein secretion system is also less complex compared to other bacteria, lacking many channel-forming proteins, possibly due to the lack of a cell wall and periplasmic space (25). Because of the truncated respiratory system and need for metabolic products, mycoplasmas have an obligate association with the host as a metabolite source. Due to this association, mycoplasmas are not usually found outside of the specific hosts and tissues they colonize (21).

Mycoplasma pneumoniae

Discovery**.** In 1944 Eaton isolated an organism from a patient with a lower respiratory tract illness that was originally termed "Eaton's agent" and classified as a filterable virus as large as 180-250μm (29, 30). Eaton's agent could be propagated in chick embryos and intransally infected into cotton rats, hamsters and other animals, resulting in the development of pulmonary lesions. But no inoculations on human volunteers with the agent propagated in chick embryos was done by Eaton at the time (29, 31, 32). It was filterable and not inhibited by antibiotics such as sulphonamides and penicillin, supporting the initial classification as a virus (33).

In 1943, the Pinehurst Trials were started, involving a series of experiments to investigate the problem of atypical pneumonia in the United States. Throat washings and sputum from patients with atypical pneumonia were used to infect volunteers. More experiments were done using either filtered (through a Corning or Seitz filter), autoclaved, or untreated samples from patients with atypical pneumonia. This study led to the conclusion that the bacteria-free filtrates, assumed to contain a virus, produced primary atypical pneumonia in human volunteers (30). This led to further study of

Eaton's Agent, including development of diagnostic tools. Sera isolated from patients with infections caused by Eaton's agent successfully inhibited growth of the organism (32, 34). In 1957 a technique was described that provided a serological diagnostic method using fluorescent-stainable antibodies related to Eaton Agent infections that proved to be specific and sensitive (35, 36). Complement Fixation (CF) tests using serum were also studied and shown to have 78 and 92% sensitivity and specificity, respectively.

Further investigation suggested that Eaton's Agent was a pleuropneumonia-like organism (PPLO), which refers to the organisms in the order *Mycoplasmatales* (37). This was the first demonstration of a PPLO associated with human respiratory disease (37). Further studies of Eaton's agent showed it to be sensitive to antimicrobial compounds such as organic gold salts, as well as tetracyclines, carbomycin, and erythromycin (33, 38-40). This was in direct conflict with its classification as a virus. When visualized on the mucous layer covering the bronchial epithelium of an infected chick embryo, it was shown to be a coccobacillary shape, similar to cells seen in exudate associated with certain pathogenic mycoplasmas (40, 41). It was demonstrated that it could be propagated in tissue culture, these tissue culture materials were then stained and visualized showing rounded granular structures (42, 43). The successful growth of Eaton's agent was accomplished in cell-free media with yeast extract and horse serum, with colonies grown on agar presenting as extremely small and "fried egg" or granular in appearance (37). These characteristics overwhelmingly suggested that the Eaton's agent was a member of the mycoplasmas, an accumulation of these studies and proposed change of nomencluature to *Mycoplasma pneumoniae* was accepted (37, 40, 44).

Disease Manifestation**.** *M. pneumoniae* is carried in the nose, throat, trachea and sputum of infected individuals (45). Infections occur both endemically and epidemically worldwide and can induce both upper and lower respiratory tract symptoms (46, 47). The organism is typically associated with desquamated epithelial cells carried in the mucus and can be transmitted efficiently via coughing. This requires close personal contact for transmission, making areas such as schools, barracks, prisons and other institutions ideal settings for passing of infections (45). Older studies showed that pneumonia caused by *M. pneumoniae* is most common in school-aged children 5 to 15 years of age, with fewer cases seen in children under 5 as well as after adolescence and into adulthood (48-50). Due to improved detection abilities, recent studies have shown that incidence may occur in children under 5 and older persons both endemically and occasionally epidemically, (49, 51-54).

M. pneumoniae infection can result in minimal symptoms that resolve quickly, or more severe and long-term complications. The most clinically important illness associated with *M. pneumoniae* is atypical pneumonia, also referred to as "walking pneumonia" (2). This is differentiated from classical pneumococcal pneumonia by its lack of response to antimicrobial therapy with sulfonamides or penicillin, as well as differing symptoms. Pneumococcal pneumonia is characterized by an acute onset and potentially severe course, with lobar involvement, while atypical pneumonias have a longer incubation with more pronounced systemic symptoms (55-57). A symptomatic disease will develop over a period of several days to weeks and can persist for weeks to months. Common symptoms include sore throat, hoarseness, fever, cough, headache, chills, earache, general malaise and coryza. Adults typically show minimal symptoms,

while children 5 to 15 years are more likely to develop bronchopneumonia (58-60). *M. pneumoniae* has also been linked to chronic obstructive pulmonary disease (COPD), in which the organisms persist and are difficult to clear from the body (61-64). Other common symptoms can include pharyngitis, sinusitis, and tracheobronchitis with a cough that is dry or productive (65-68). Infections can also lead to immunosuppression or alteration of respiratory tract flora, which can lead to the exacerbation of subsequent respiratory virus or bacterial infections such as *Streptococcus pyogenes* and *Neisseria meningitides* (1).

M. pneumoniae infection can also lead to extra-pulmonary manifestations, with around 25% of people infected experiencing these complications at variable time periods. There have been documented cases of *M. pneumoniae* in blood, synovial fluid, cerebrospinal fluid, pericardial fluid, and skin lesions (69-72). Neurological complications appear in 6-7% of hospitalized patients with confirmed cases, and cardiac complications in up to 8.5% of cases. There has also been a link between *M. pneumoniae* infections and new-onset asthma, persistent and worsening asthma, and exacerbation of asthma (73-75). It has been shown to exacerbate symptoms of asthma alone or in combination with other respiratory infections, with 18% of hospitalized asthmatics having *M. pneumoniae* infections (76-78). The release of proinflammatory cytokines associated with mycoplasma infection is the implicated mechanism for asthma exacerbation (79-81). *M. pneumoniae* can lead to many respiratory complications, including chronic diseases, while also causing extra-pulmonary issues. However, incidence of infection is commonly misperceived as rare, due to lack of effective tools for diagnosis (1).

Cell Biology

Cell Morphology. *M. pneumoniae* is a pleomorphic organism, typically elongated with a polarized knob-like protrusion known as the terminal or attachment organelle (82). Cells can vary in length from 1-5um and 0.1-0.3um wide (82). When grown on glass or plastic surfaces over the span of days, *M. pneumoniae* has been shown to produce colonies of varying size, as well as a web like pattern of filamentous forms (82, 83). Colonies on agar are homogenous and granular in appearance and 10-100um in size (37). When in colonies, cells have been shown to be both elongated and flask-shaped, as well as rounded (82, 84).

Terminal Organelle. *M. pneumoniae* has a unique terminal organelle that is 300nm long and 90nm wide (82). The terminal organelle is made up of a proteinaceous electron-dense core and various membrane proteins (Fig. 1). The proteins of the terminal organelle are encoded by nine genetic loci (17, 85-87). The role these proteins play in the terminal organelle have been elucidated by various mutant studies, but how some of these proteins carry out these roles is still not clear.

The electron-dense core takes up most of the volume of the terminal organelle and is often oriented along the long axis of the cell (88). It consists of a bowl complex, rods, terminal button at the tip of the organelle, and protein knobs on the cell surface (89-92). The proteins HMW1 and HMW2 are believed to make up the thin and thick parallel rods, respectively (87, 93-95). HMW1 has been shown to localize exclusively to the terminal organelle and is required for the presence of the electron dense core (96). Mutants of HMW1 or HMW2 have been shown to lack an electron-dense core, as well as other substructures (85, 93, 97, 98). Loss of HMW1 or HMW2 also impacts the stability or

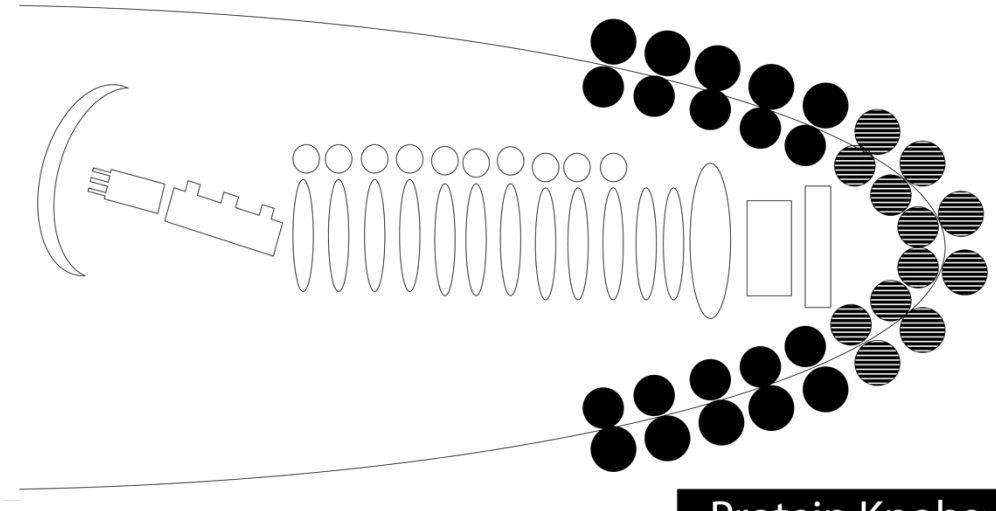

Paired segment rods, terminal button, Bowl Complex

Protein Knobs: P1, P40, P90

P1, P40, P90, P30

Figure 1. Terminal organelle schematic. Schematic of *M. pneumoniae* terminal organelle architecture. Adapted from Krause et. al 2018.

synthesis of one another, and impacts stability of HMW3, P65, P41, P30 and P24 as well (8, 97, 99-102).

The terminal button is comprised of three subunits and is found adjacent to the complexes that line the inner surface of the terminal organelle membrane (98). Protein HMW3 exists as polymerized filaments surrounding the core at its distal end, where the terminal button is located. The loss of HMW3 reduces levels of P65, another protein associated with the terminal button, resulting in decreased cytadherence, gliding, and localization of P1 to the terminal organelle (96, 98, 103). Protein P65, located at the distal end of the terminal organelle, is partly surface exposed and requires HMW3 and P30 for optimal stability and localization (104-108). Studies have shown that the absence or mutation of P65 impacts cytadherence, gliding motility, and surface dynamics of P30 (109).

The bowl complex at the base of the terminal organelle acts as an anchor between the terminal organelle and cell body and is made up of four substructures involving the P41, P24, TopJ, and MP387 proteins (5, 7, 87, 110). A mutant of the P41 protein shows the presence of all substructures except the bowl complex (98), but results in a unique phenotype in which the terminal organelle pulls away from the cell body, detaching, and continuing to glide independently (111). Protein P41 is either a component of the bowl complex or is required for the assembly or stability (110, 112). Protein P41, along with P24, function in some role related to gliding initiation and wild type level gliding frequencies while also playing a role in formation of new terminal organelles at a wild-type rate (110, 112).

The cell surface of the attachment organelle has protein knobs, distanced 16 to 26nm apart, that are involved in interaction of the cell with surfaces (91, 92, 95). Protein P1 is responsible for binding to solid surfaces, use of monoclonal and polyclonal antibodies against P1 result in inhibition of cytadherence, and has been shown to correspond to the nap seen in electron micrographs (8, 87, 113-116). Proteins P90 and P40, cluster at the terminal organelle but are present at lower concentrations throughout the entire cell (93, 96, 99, 106, 117-119). These proteins are required for gliding motility and are stabilized by the protein P1(120, 121). Studies suggest that protein P1, in complex with P90 and P40, and possibly P30, forms these protein knobs (93, 95, 122). P1 is also involved in gliding motility, functioning as the "legs" of gliding, with monoclonal antibodies decreasing gliding speed over time and removing gliding cells from a glass surface (123). The DnaJ-like co-chaperone TopJ plays a role in protein knob density, and mutants lacking TopJ show a low abundance of protein knobs, which appears to be due to poor processing of P1 to the membrane (7, 124).

Protein P30 is a transmembrane protein at the distal end of the terminal organelle, with no detection elsewhere on the cell (93, 96, 106, 125). P30 is also an important player in gliding, with mutations in P30 resulting in irregular morphology, inability to glide, and a reduction in protein knob density (3, 98, 113, 126, 127). P30 may be required for P1 stability in the appropriate conformation in the membrane, P30 mutants result in properly localized but nonfunctional P1 (3, 126). Studies suggest that P30 may be the link between these protein knobs and the force-generating mechanism of gliding motility in *M. pneumoniae* (123, 126).

Gliding Motility**.** *Mycoplasma pneumoniae* has a unique gliding motility that is necessary for colonization of host cells (9-11, 128, 129). Previous work with terminal organelle mutants that have impaired gliding motility revealed reduced colonization of normal human bronchial epithelial (NHBE) cells and mice models (5, 6, 10). The P30 mutant, II-3, has a frameshift due to the loss of a single adenine nucleotide in the MPN453 gene that leads to lack of detectable P30 (Fig.2) (3). The P30 mutant has been shown to have an altered cell morphology as well as reduced capacity for binding to erythrocytes and non-motility (Fig. 3) (3, 126). This mutant was determined to be avirulent in BALB/c mice and unable to colonize NHBE cells at wild-type levels (6, 10). The II-3R revertant has a second-site mutation that restores the reading frame of MPN453, but alters 17 residues in the P30 protein sequence (Fig. 2), restoring adherence to 60% wild-type levels but has a reduced gliding speed of 5% compared to wild-type (126). The II-3R mutant has also been shown to be avirulent in BALB/c mice and cannot be recovered from the lungs of mice post infection (6). Another P30 mutant, II-7, which has a truncated P30 and reduced attachment as well as gliding speed, also colonized NHBE cells at a lower rate (10, 130) The P200 mutant, which is able to attach but has impaired gliding motility, colonizes NHBE cells at a lower rate compared to wild type (5). Loss of TopJ, a molecular chaperone, also affects the terminal organelle by impairing the final P1 product, which leads to deficiency in attachment and loss of motility (7, 124, 131). These mutant studies emphasize the importance of a functional terminal organelle, which is responsible for the repeated binding to receptors on solid surfaces that allows for this motility to occur (123, 126).

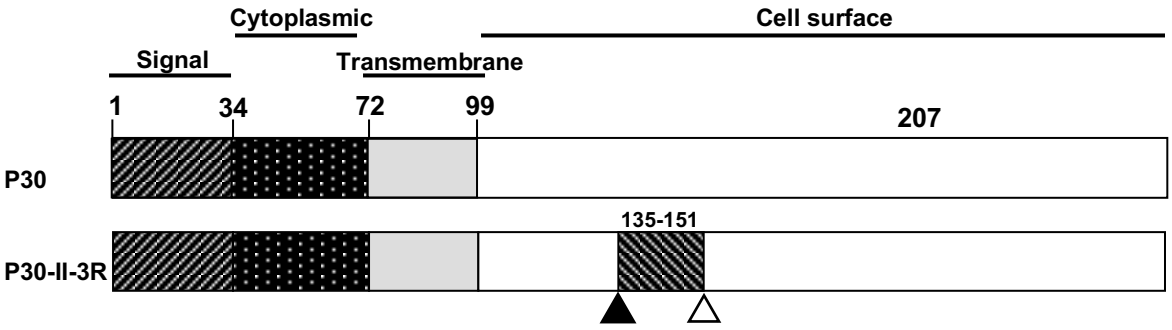
Cytoplasmic
Cell surface
Signal
Transmembrane
1
34
72
99
207
P30
135-151
P30-II-3R

Figure 2. *M. pneumoniae* P30 mutants Cytadherence-associated protein P30 in wild-type M. pneumoniae and P30 mutants II-3 and II-3R. For P30-II-3R, a frameshift (open triangle) resulted in mutant II-3 with no detectable P30. A second site mutation (solid triangle) in revertant II-3R restored P30 except for residues 135-151. Adapted from Hasselbring, et. al 2005.

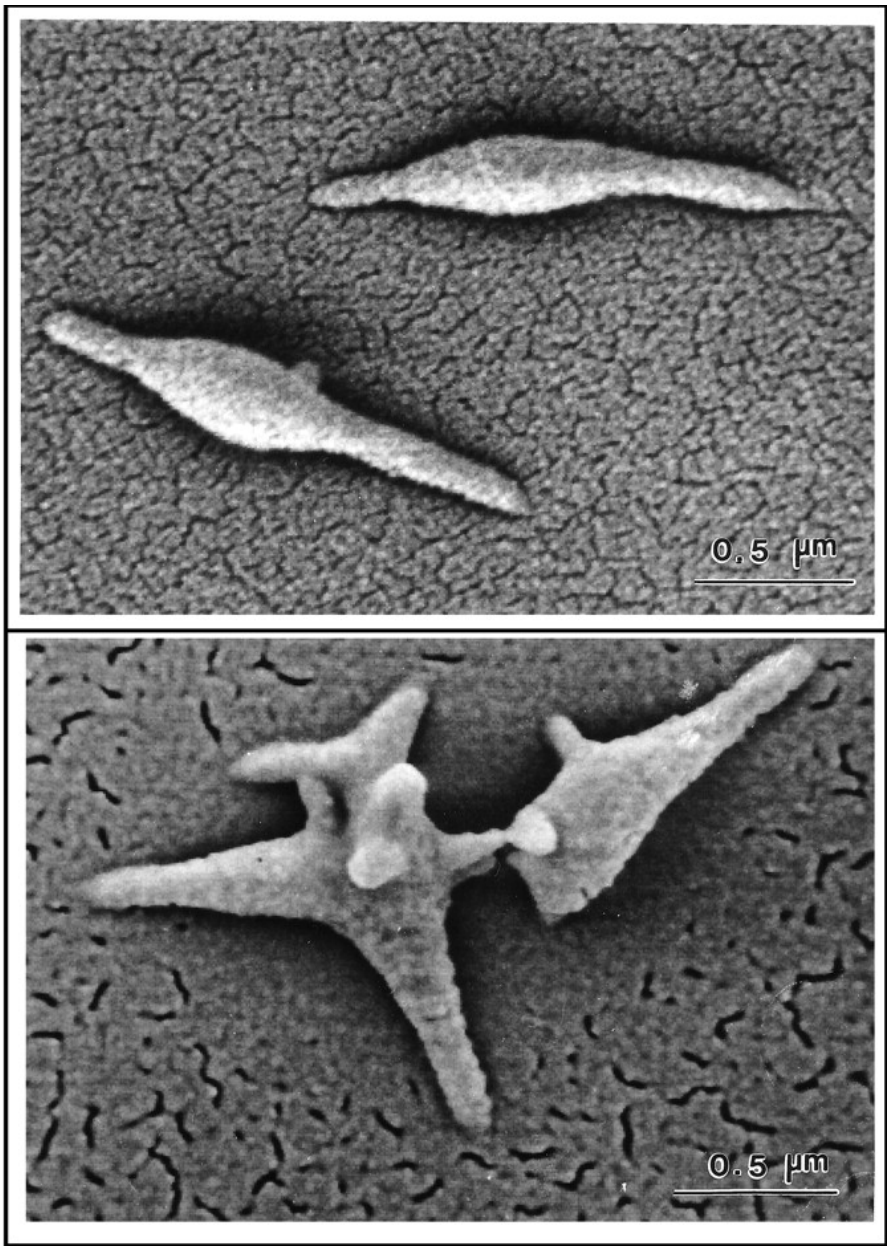

Cynthia E. Romero-Arroyo et al. J. Bacteriol. 1999;181:1079-1087

Figure 3. P30 mutant cell morphology. High-magnification SEM images of wild-type *M. pneumoniae* (A) and P30 mutant II-3 (B).

The P1 adhesin complex is the key player in gliding motility, serving as the "leg" (123). The P1 adhesin complex is found on the surface of the terminal organelle and has been seen by electron cryotomography, appearing as knob like structures 4-8nm in length and 8nm in diameter (91, 92). The current suggested gliding mechanism starts with the P1 adhesin binding to sialylated oligosaccharides (129). The electron dense core then causes elongation of the attachment organelle, extending it. The P1 adhesin then detaches from the receptor, the core compresses again, and the process repeats in a "catch and release" mechanism (129). Other mycoplasmas, such as *M. mobile* and *M. genitalium*, do possess terminal organelles and utilize gliding motility. However, the mechanisms for gliding are not the same, and the terminal organelles between species are very different, having come about by convergent evolution (86, 129, 132, 133).

The energy source of many bacterial motility systems is based on membrane potential, with some such as pili-based motility utilizing ATP for energy (134). The terminal organelle has been shown to be the motor for gliding motility (97, 111, 123, 126) with previous studies determining the gliding speed of *M. pneumoniae* to be 0.3-4 μm/second (105, 135). In *M. mobile* the energy source has been shown to be provided by ATP, cellular "ghosts" with damaged membranes were reactivated with the addition of ATP (11, 136, 137). Similar experiments with *M. pneumoniae* were unsuccessful. However, studies have shown that disruption of the Ser/Thr protein kinase gene or the cognate protein phosphate gene, referred to as the *prkC* and *prpC* mutants respectively, does alter gliding speed and frequency (120, 138). Deletion of these genes also results in alteration of phosphorylation levels of the component proteins in the attachment organelle, which in turn affects gliding motility. However, PrpC and PrkC are not the

sole force driving the gliding motor, and it is suggested that motility may be a cellular process controlled by reversible Ser/Thr phosphorylation (139, 140).

Mycoplasma pneumoniae Pathogenesis and Host Interaction

Pathogenesis. *M. pneumoniae* invades host tissues during infection and has been shown to invade cells in some cell lines (10, 141, 142). The terminal organelle positions the mycoplasmas in close proximity to host cells, helping to facilitate localized tissue disruption and cytotoxicity (143-145). Cytadherence of *M. pneumoniae* to host cells is the initiating event in disease production and is considered to be a major virulence factor, mutants deficient in attachment have been shown to be avirulent (3, 5-8, 128). Gliding motility has also been shown to be an important factor during infection, with gliding deficient mutants exhibiting reduced colonization of mice and tissue culture models (9-11). Tissue culture studies have shown that after attachment to the cilia tip, *M. pneumoniae* will glide from the tip to the surface of the cell and subsequently spread, eventually leading to pericellular invasion (127, 146). During infection *M. pneumoniae* parasitizes mammalian cells through deterioration of cilia and vacuolization of cells (45). Host cell metabolism is also impaired by reduction of oxygen consumption, glucose utilization, amino acid uptake and macromolecular synthesis (2).

Infected tissue in the human host is damaged through the production of reactive oxygen species (ROS), hydrogen peroxide and superoxide radicals (2). These ROS act along with endogenously created ROS to create oxidative stress in respiratory epithelium (45). As the ROS inhibit catalase in the host cells, breakdown of peroxides produced by *M. pneumoniae* and host cells is reduced, rendering the host susceptible to oxidative damage (2). Production of ROS serves as an important virulence factor for *M.*

pneumoniae and confers its hemolytic activity (147). Initial catalase activity by the host was shown to initially inhibit infection in the murine respiratory pathogen *Mycoplasma pulmonis*, but the catalase actually enhanced the presence of the organism later in life (148). A similar phenomenon was shown by Dybvig, et al. where addition of catalase to *M. pneumoniae* cultures showed a beneficial impact on growth (149). *M. pneumoniae*, as well as other mycoplasma species, have been shown to form biofilms (150-156). The addition of catalase was shown to enhance biofilm formation, this is likely due to the inactivation of hydrogen peroxide and its oxidative effects (149). However, the structure of the biofilm is also altered by the addition of catalase. Grown without catalase, *M. pneumoniae* biofilms formed more tower structures compared to a smoother more homogenous biofilm when grown with catalase (149). Formation of biofilms allows for protection against complement components, peptide antimicrobials, and as a mechanism for coping with endogenous sources of hydrogen peroxide (149, 154).

M. pneumoniae also produces an exotoxin, known as the community-acquired respiratory disease syndrome (CARDS) toxin (157). The CARDS toxin carries significant sequence homology to the pertussis toxin S1 subunit and carries out an ADP-ribosylating activity. It has been shown to bind to human surfactant protein A and annexin A2 on airway epithelial cells (157). The CARDS toxin binds to mammalian cell surfaces and is internalized through a clathrin-mediated pathway (158). The toxin causes vacuolation and ciliostatis in cultured host cells (157). The close proximity of bacteria to host cell allows for *M. pneumoniae*-produced ROS and CARDS toxin to damage host cells in various ways.

Immune Response**.** *M. pneumoniae* infection in the human host initiates a robust immune response that is typically ineffective, and re-infection can be common (2, 12). *M. pneumoniae* is able to evade or modulate the host immune response through immunomodulatory activities such as molecular mimicry of proteins and glycolipids of mammalian tissues. In particular, the P1 adhesin gene undergo rearrangement by recombination with repeat elements throughout the genome leading to antigenic variation, making it difficult for the host immune response to target (159, 160). The host immune system mounts a pro-inflammatory response in the presence of *M. pneumoniae* lipoproteins on the cell surface, cytadherence, and the CARDS toxin. This leads to activation of toll-like receptors, release of cytokines, and activation of the inflammasome (161). During infection, cytokines and lymphocytes are produced, which may exacerbate or minimize disease. This response may enhance host defense mechanisms to minimize disease or create immunological lesions leading to an exacerbation of disease. A more vigorous cell-mediated immune response can create more severe clinical disease (45). When infection occurs, the host immune response activates macrophages, which undergo chemotactic migration to the infection site. Neutrophils and lymphocytes are present in alveolar fluid, and white blood cells infiltrate the lung (162, 163). The host's T-cell mediated immune response leads to lymphocyte blast transformation in those previously infected, as well as a chemotactic response of leukocytes when *M. pneumoniae* is present (164-166).

M. pneumoniae infections often begin with a long incubation period before symptoms appear and an antibody response becomes evident. The antibody response is elicited by protein and glycolipid antigens, with P1 being the target of many antibodies

(45). The immune system responds by producing antibodies that peak after three to six weeks of infection, with a gradual decline over months to years (45). Within one week of initial infection IgM specific to *M. pneumoniae* appears, followed by IgG two weeks later (167, 168). IgM may persist for months to years following infection. Early during infection antibody IgA is produced in serum but peaks quickly (169, 170).

Despite the host's robust immune response *M. pneumoniae* infection can be difficult to clear completely, leading to chronic respiratory problems (49). Work by Hardy et. al. studied chronic infection of *M. pneumoniae* in a murine model using BALB/c mice (171). Mice were inoculated intranasally and examined post infection starting at 108 days and ending at 530 days. *M. pneumoniae* was detected by polymerase chain reaction and culture in 22% of mice at 530 days, compared to 70% at 108 days (171). However, at 530 days 78% of infected mice demonstrated abnormal histopathology characteristics associated with chronic infection (171). An early report by Meakins showed extended stay recovery for some individuals with primary atypical pneumonia, indicating a similar phenomenon in human cases of chronic infection (172).

Glycan Receptors**.** During infection *M. pneumoniae* attaches to glycan receptors on the surface of the host cell. Specifically, it has been shown that *M. pneumoniae* attaches to sialic acid containing glycoproteins (173-177). Treatment of these proteins with neuraminidase, an enzyme that cleaves terminal sialic acid linkages, results in a loss of adhesion activity. This has been shown with various cell types, such as hamster tracheal rings, where neuraminidase treatment results in lower levels of attachment (16, 144). Studies conducted with sialylated glycoprotein-coated glass showed a specificity for sialic acid linked α-2,3 to galactose (15). Proteins with the α-2,3linkage such as

laminin, fetuin, and human chorionic gonadotropin (HCG) promote adhesion, while proteins with alpha 2-6 linkage do not (15). α-2,3 sialic acid linked to galactose has been found on non-ciliated bronchiolar cells at junctions between respiratory bronchiole and alveolus (178). Treatment of these α-2,3 sialylated glycoproteins with neuraminidase inhibited attachment (15).

Other studies have shown that free α-2,3 sialyllactose in the medium also inhibits binding to sialylated glycoproteins on a surface (15, 17). Binding of *M. pneumoniae* appears to be sensitive to the structure of the oligosaccharide in a "lock and key" manner, with the most effective binding occurring to Neu5Ac- α-2,3-lactosamine (17). This structure is found in the lower part of the human trachea, and has been shown to be present on human bronchial epithelium on ciliated cells (179-181). Numerous studies have shown that sialylated receptors play an important role in *M. pneumoniae* attachment to host epithelial cells.

Sialylated receptors are not the only glycan used in attachment, as *M. pneumoniae* also attaches to sulfated glycolipids. Attachment was observed on glycolipids with a Gal($3SO_4$)β1 residue, as well as an isomer of sulfatide with the sulfate in the 6-position (14). However, sulfate itself was shown not to be sufficient for binding alone, as *M. pneumoniae* did not attach to cholesterol sulfate or sulfated glucoronosylparagloboside (14). Specificity for sulfatide attachment was demonstrated by competition with dextran sulfate, which inhibited binding to sulfatide and to host cells (14). Binding of *M. pneumoniae* to sulfatide was shown to be energy-and-temperature dependent, indicating a need for metabolic activity for attachment to the receptor (14). Sulfatide has been shown

to occur in high amounts in human trachea and human lung, giving physiological relevance to *M. pneumoniae* attachment to the sulfated glycolipid (14).

Previous studies of *M. pneumoniae* have elucidated the role of temperature and energy in cell attachment. Incubation of *M. pneumoniae* on the sulfated glycolipid, sulfatide, at varying temperatures of 4°C to 37°C showed a decrease in attachment at 4°C compared to 37°C (14). The addition of various metabolizable sugars, such as glucose, as well as their catabolic products, like pyruvate, have shown an enhancing effect on attachment (182). Treatment of cells with certain metabolic inhibitors does impact attachment levels. Proton motive force inhibitors such as carbonylcyanide m-chlorophenylhydrazone and 2,4-dinitrophenol reduce attachment, by either uncoupling metabolic energy from substrates crossing the membrane or inducing conformational changes in membrane proteins (183, 184). Overall, it has been suggested that a cell must be metabolically active to attach and infect respiratory epithelium (144, 175), indicating a direct relation between attachment and metabolic energy.

Both the sialylated and sulfated receptors are not specific to just *M. pneumoniae* but have been shown as receptors for other mycoplasma species. *Mycoplasma mobile*, a fish pathogen, utilizes a similar sialylated receptor to *M. pneumoniae*, α-2,3 and α-2,6 N-acetylneuraminyllactose. Both receptors inhibit blinding of *M. mobile* to glass during gliding, in a concentration-dependent manner (179). *Mycoplasma gallisepticum*, a poultry pathogen, has also shown specificity for sialylated receptors. Removal of sialic acid from red blood cells by neuraminidase treatment resulted in decreased attachment of *M. gallisepticum* (185). *Mycoplasma hominis*, a human pathogen found in the urogenital tract, binds to sulfatide, with inhibition of attachment occurring in the presence of dextran

sulfate (186). The notable porcine pathogen *Mycoplasma hyopneumoniae* has also been shown to bind sulfatide, with effective inhibition of attachment with dextran sulfate treatment (187, 188). While there are many similarities between receptors of the mycoplasmas, no species have been shown to utilize the exact same set of receptors.

Just as the mycoplasma species show some similarities in receptor preference, many notable respiratory pathogens also use sulfated or sialylated receptors. *Bordetella pertussis,* the causative agent of whooping cough, has been shown to bind to sulfatide in a dose-dependent manner. Only virulent strains bind to sulfatide, and inhibition of binding with dextran sulfate has been shown (189). Another bacterium that causes pneumonia, *Streptococcus pneumoniae,* has been shown to rely on oligosaccharides with α-2,3 or α-2,6 sialylated linkages for adherence to epithelial cells (190). Most notably, the influenza virus binds to sialic acid-containing molecules (191). The avian influenza target is the same as *M. pneumoniae*, Neu5Ac-α-2,3-lactosamine, while the human influenza target is the same as *M. mobile*, Neu5Ac- α-2,6-galactose (179). Interestingly, the virus is able to cleave sialic acid to free itself from binding to receptors that do not lead to viral infection through a neuraminidase surface protein. These surfaces may include dead cells, other virions, and respiratory secretions (191). *M. pneumoniae* glycan receptors are not only important for its own infection but also other mycoplasma species and notable respiratory pathogens.

Lectin Biochemistry

At the heart of this dissertation is the interaction of *M. pneumoniae* surface proteins with specific glycan structures. There are a diverse number of carbohydrates on cell surfaces, these structures can be bound by proteins, termed lectins (192, 193). These

lectins can bind monosaccharides as well as oligosaccharides, termed ligands (194). Lectins can bind reversibly and with specificity, they have no enzymatic activity and are produced by the immune system (194). Lectins are found throughout the tree of life from animals to microbes and facilitate various cell-to-cell interactions (192, 193). These interactions can promote adhesion of pathogens as well as intracellular trafficking of glycoproteins and cell interactions in the immune system, among other things (194). For example, some pathogens like *M. pneumoniae* and influenza, utilize carbohydrates on host cell surfaces as receptors for attachment (14, 15, 178).

The binding energies of these protein-carbohydrate interactions tend to be lower than that of protein-protein interactions but can be highly specific (192). When observing these lectin-carbohydrate complexes, evidence has shown that hydrogen bonds and van der Waals interactions contribute to the binding energy between the two (192, 194, 195). The interaction of lectins and monosaccharides are relatively weak and can have a more relaxed specificity, compared to that of oligosaccharides (194-197). These oligosaccharides could have clusters of binding sites, multiple branches, and various spacing of binding sites that allows for multiple interaction points between the lectin and the ligand compared to an individual monosaccharide (194). However, the avidity of monosaccharide interactions can be increased through multiple lectin-ligand interactions (198-200). These multivalent interactions in biological systems enhance weak interactions and are used in processes such as viral entry and host-pathogen interactions (198).

Lectins may be specific for a single monosaccharide or oligosaccharide. For monosaccharide specificity, affinity may or may not change based on what other sugars

are linked to that monosaccharide. Conformational flexibility allow some lectins to interact with a wide range of sugars, while these may allow for more overall interactions it can reduce the affinity and specificity of the interaction (201). But, as mentioned previously the interaction of the lectin with multiple receptors can increase affinity. So, a monosaccharide linked to sugars that are also recognized by the lectin to some extent can increase the affinity of the overall interaction (195, 202). Specificity of these interactions can be affected by hydrogen bonding, shape complementarity, charge distribution and conformational flexibility (201). To achieve the highest possible affinity the surface of each lectin and ligand would have to be mirror images, as well as having complementing charge distributions on the surface (201). The particular sugar functionalities that form hydrogen bonds with the lectin are required for specific recognition and discrimination, while other elements that are typically not in contact with the protein are not used (195). Overall, protein-carbohydrate interactions play a major role in biological processes across the tree of life. These interactions can be highly specific or more relaxed and vary in their affinity.

CHAPTER 3

MATERIALS AND METHODS

M. pneumoniae culture

I grew *M. pneumoniae* wild-type strain M129 (203) for seventy-two hours at 37°C in tissue culture flasks in SP4 medium (204) containing fetal bovine serum (FBS). For comparison with the non-attaching mutant strain II-3 (205), wild-type, mutant and revertant cultures (II-3 and II-3R) were grown in glass bottles coated with 0.1% poly-l-lysine (Sigma-Aldrich) to promote attachment. When cultures reached mid-log phase (pH 6.9-7.1), the growth medium was removed and the culture vessels were washed three times with phosphate buffered saline (PBS; pH 7.2). Mycoplasmas were then scraped from the surface into PBS and harvested by centrifugation at 20,000 × *g* for twenty minutes at 4°C. The resulting pellets were washed once with PBS by centrifugation, suspended in modified SP4 medium (mSP4; no FBS and phenol red), plus 5% ovalbumin (Sigma-Aldrich), syringe-passaged ten times using a 25-gauge needle to disperse the cells, and syringed-filtered twice (0.45μm) to remove cell clumps.

Preparation of glycoprotein-coated substrates

Four-well chambered coverglasses (#1; Nunc Lab-Tek) treated with receptor preparations at varying concentrations were utilized for all binding assays. The receptor substrates tested were the sialoglycoproteins murine laminin (Invitrogen) and human chorionic gonadotropin (hCG; Sigma-Aldrich). Laminin and hCG were dissolved individually in PBS at concentrations ranging from 0.2-50 μg/ml and incubated in 500-μl

volumes per chambered coverglass well for one hour at room temperature. As a positive control for *M. pneumoniae* binding, chambered coverglasses were incubated with SP4 medium for one hour at room temperature to allow FBS glycoproteins to coat the coverglass surface (82). Receptor solutions were then removed, all wells were washed once with PBS, and 5% ovalbumin (Sigma-Aldrich; ≥ 98% purity) was added for one hour at room temperature to limit nonspecific binding of *M. pneumoniae* to the glass. As a negative control for *M. pneumoniae* binding, chambered coverglasses were pre-incubated with 5% ovalbumin alone for one hour at room temperature. For neuraminidase treatment, 0.5 units of neuraminidase (Sigma-Aldrich) was incubated for one hour at 37°C in PBS, then removed and chambered coverglasses washed with PBS before inoculation with *M. pneumoniae*.

Preparation of sulfated glycolipid substrates

Four-well chambered coverglasses pre-treated with sulfated glycolipid sulfatide at varying concentrations were utilized for all binding assays. Sulfatide was dissolved in chloroform:methanol:water (8:3:2) for storage at -20°C. Prior to use the chloroform:methanol:water (8:3:2) was evaporated under a stream of nitrogen and the sulfatide dissolved in methanol:water (1:1), at concentrations ranging from 0.2-20 μg/ml. Sulfatide solutions were incubated in 500-μl volumes per chambered coverglass well for two hours at room temperature. As a positive control for *M. pneumoniae* binding (82), chambered coverglasses were incubated with complete SP4 medium for one hour at room temperature. Receptor solutions were then removed, all wells were washed once with PBS, and 5% ovalbumin (Sigma-Aldrich; ≥ 98% purity) was added for one hour at room temperature to limit nonspecific binding of *M. pneumoniae* to the glass. As a negative

control for *M. pneumoniae* binding, chambered coverglasses were pre-incubated with 5% ovalbumin alone for one hour. For inhibition studies, 10ul of a 20mg/ml solution of dextran sulfate (Sigma Aldrich; 500,000MW) was added to each concentration with the *M. pneumoniae* culture.

Preparation of chemically functionalized surfaces and determination of sialyllactose density

All glass coverslip substrates with grafted poly(PFPA) brushes were fabricated as described previously (206). Hydrazide linkages for conjugating reducing sugars to the poly(PFPA) were generated by incubating the poly(PFPA)-grafted substrates in trimethylamine and anhydrous dimethylformamide (DMF) containing hydrazine monohydrate (206). We controlled the density of hydrazide linkers by replacing various percentages of hydrazine with ethanolamine hydrochloride. These were allowed to react with the poly(PFPA) substrates for two hours at room temperature, rinsed with DMF, and dried under a stream of nitrogen. To conjugate the sialyllactose, the disaccharide sodium salt (Carbosynth) (10 mM) and aniline (100 mM) were dissolved in 100 mM sodium acetate buffer (pH 4.5). The hydrazine/ethanolamine-modified substrates were incubated with the sialyllactose solutions in a moisture chamber for twenty-four hours, rinsed with water, and dried under a stream of nitrogen. Surface characterization was carried out as described previously and included ellipsometry, drop shape analysis, and Fourier transform infrared spectroscopy for thickness, hydrophobicity and chemical changes of the thin polymer film (206). Neuraminidase (Sigma-Aldrich) treatments were done for one hour at 37°C, using 0.5units per well for all assays, following sugar functionalization.

To quantify the percentage of hydrazide on poly(PFPA) surfaces, coverslips prepared in parallel were incubated with *p*-nitrobenzaldehyde (0.03 mmol) dissolved in DMF/water (1:1 vol/vol) and then aniline (0.3 mmol) and the pH adjusted to 4.5 with 2 M HCl. After two hours, the substrates were rinsed with DMF, water, DMF again, and then dried under a stream of nitrogen. The absorbance of conjugated *p*-nitrobenzaldehyde on each quartz substrates was measured by UV-vis spectrometry and surface hydrazide percentages calculated by comparing the absorbance of hydrazine/ethanolamine-modified substrates with that of substrates modified with 100% hydrazine, based on an extinction coefficient for *p*-nitrobenzaldehyde of 23283±59 $M^{-1} \cdot cm^{-1}$ at 330 nm.

Analysis of *M. pneumoniae* binding and gliding

M. pneumoniae cell suspensions of 10^7-10^8 color-change units in 600-µl volumes were prepared as described above and added to each pre-treated chambered coverglass well and incubated one hour at 37°C (207). The culture medium was removed, each well was washed three times with mSP4 to remove unattached mycoplasmas, and 600 µl mSP4 plus 3% gelatin was added per well. We examined coverglasses by using a DM IRB inverted microscope (Leica Microsystems) and captured images with a digital charge-coupled-device camera (Hamamastsu Photonics K.K.). Images were analyzed using Openlab version 5.5.0 (PerkinElmer). We quantified binding by direct microscopic counts from phase contrast images. For direct microscopic counts, we analyzed 10 fields of view from three replicates, counting only individual mycoplasma cells and excluding occasional clumps of cells. We assessed gliding motility as described previously (126). Briefly, we captured time-lapse movies for mycoplasma cultures maintained at 37°C in an incubator chamber surrounding the microscope (Solent Scientific). We calculated

gliding speed for individual cells over a minimum of 20 uninterrupted frames at a constant time interval along a collision-free cell path, with paths tracked using Openlab software. We used those measurements to calculate average gliding frequency for a minimum of 200 cells, and gliding speed for a minimum of 100 cells, per experimental treatment per experiment. Results are presented as the means and positive standard errors of the mean for each treatment from three independent experiments.

Statistics

Data on cell attachment and gliding percentage were analyzed in SigmaPlot (systat Software) by multivariate analysis of variance followed by Holm-Sidak post hoc pairwise comparisons.

CHAPTER 4

RESULTS

M. pneumoniae binding to sialylated glycoproteins

We examined binding of *M. pneumoniae* to laminin and hCG to provide a baseline for subsequent gliding analysis. In collaboration with the Complex Carbohydrate Research Center at the University of Georgia, we detected 16.5-19 and 3.2 mol sialic acid per mol of laminin and hCG, respectively, by high performance anion exchange chromatography coupled with pulsed amperometric detection (HPAEC-PAD) (data not shown). *M. pneumoniae* bound to chamber slides coated with laminin in a concentration-dependent manner, as expected, with saturation consistently at 10 μg (Fig. 4A and data not shown). Mycoplasma attachment to laminin at the highest levels tested was comparable to that with chamber slides pre-treated with SP4 growth medium glycoproteins, which served as a positive control. As a negative control, we used chamber slides pretreated with ovalbumin alone (Fig. 4A), for which HPAEC-PAD analysis detected only 0.5 mol sialic acid per mol (data not shown). As expected (15), *M. pneumoniae* also exhibited concentration-dependent attachment to hCG (Fig. 4B), but with saturation evident at 5 μg, and attachment levels significantly lower than for the SP4 positive control or for laminin. Pre-treatment of coated chamber slides with neuraminidase to cleave terminal sialic acid residues resulted in 50-75% reductions in *M. pneumoniae* attachment to both laminin and SP4 ($P < 0.001$), consistent with a binding specificity for sialic acid moieties, as expected (Fig. 5) (15, 208).

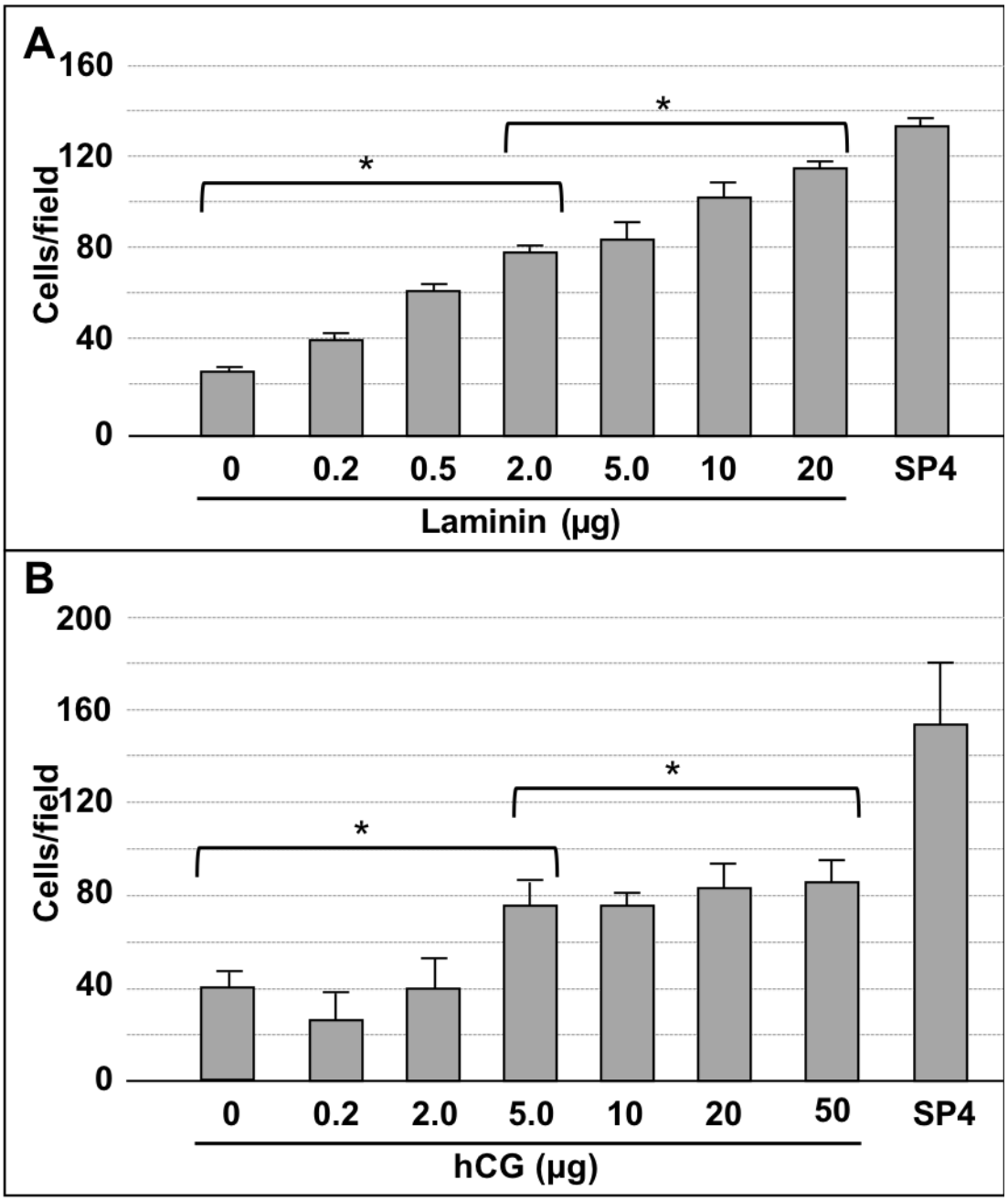
A
160
120
80
40
0
Cells/field
*
*
0
0.2
0.5
2.0
5.0
10
20
SP4
Laminin (µg)
B
200
160
120
80
40
0
Cells/field
*
*
0
0.2
2.0
5.0
10
20
50
SP4
hCG (µg)

Figure 4. ***M. pneumoniae* attachment to sialylated glycoproteins.** *M. pneumoniae* attachment to chamber slides coated with laminin (**A**) or hCG (**B**) at the indicated levels. Each bar represents the mean and positive standard error of the mean for total cell counts for three separate experiments. SP4, data for chamber slides coated with serum glycoproteins in SP4 growth medium, which served as a positive control. * $P < 0.001$ for 2.0, 5.0, 10, and 20 μg laminin relative to the 0 μg control; ** $P < 0.001$ for 5.0, 10, 20, and 50 μg hCG relative to the 0 μg control; *** $P < 0.001$ for 50 μg hCG relative to the SP4 control.

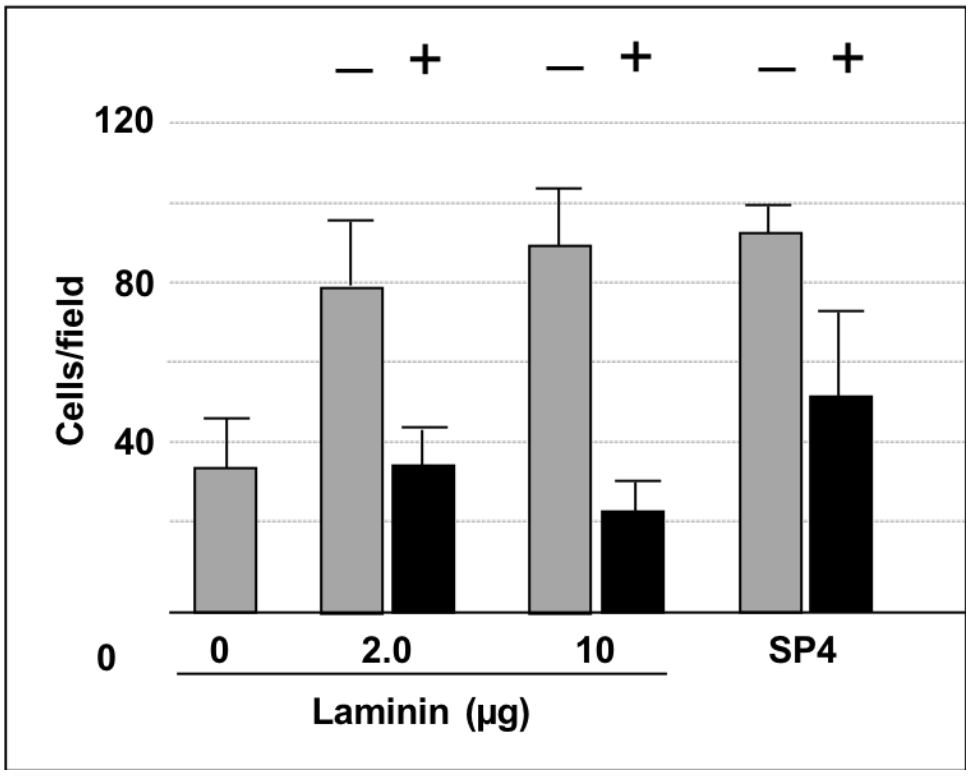
– +
– +
– +
120
80
40
0
Cells/field
0
2.0
10
SP4
Laminin (µg)

Figure 5. **Effect of neuraminidase treatment of sialylated receptors on attachment.** *M. pneumoniae* attachment to chamber slides coated with laminin, with and without pre-treatment with neuraminidase. Each bar represents the mean and positive standard error of the mean for attached cells for three separate experiments. SP4, data for chamber slides coated with serum glycoproteins in SP4 growth medium, which served as a positive control. + / -, with or without neuraminidase pre-treatment ($P < 0.001$).

M. pneumoniae gliding on laminin requires a receptor density threshold

We examined *M. pneumoniae* gliding frequency and speed on glass surfaces coated at increasing levels with laminin or hCG. We consistently observed no gliding on laminin at levels below 2 μg (Fig. 6), or on hCG at all levels tested, despite the significant attachment noted in Fig. 4. Gliding was observed on laminin at 2 μg and higher, and gliding frequency increased with laminin from 2 to 5 μg and remained at statistically similar levels at 10 and 20 μg, yet significantly higher than for the SP4 positive control (Fig. 6; $P < 0.01$). Finally, gliding speed was consistently 0.32-0.34 μm/sec for all laminin concentrations where we observed gliding, as well as for the SP4 control (Table 1).

Carbohydrate Surface Functionalization

Laminin and related sialylated glycoproteins provide a convenient but imprecise model for the study of *M. pneumoniae* interactions with airway glycans due to variability in the extent and nature of their glycosylation, and thus the inability to control oligosaccharide density, presentation, and composition limits its modeling value. Kasai et al. (17) had excellent success analyzing glycan specificity based upon the inhibitory activity of synthesized oligosaccharides in solution on mycoplasma binding and gliding on an inert surface coated with serum glycoproteins. Here we sought instead to examine mycoplasma binding and gliding activity on surfaces having well-defined oligosaccharide presentation. We recently described the use of hydrazide conjugation to ligate reducing sugars to poly(PFPA) (pentafluorophenylacrylate)-grafted surfaces (206). By varying the ratio of hydrazine and ethanolamine in the conjugation, it was possible here to control the

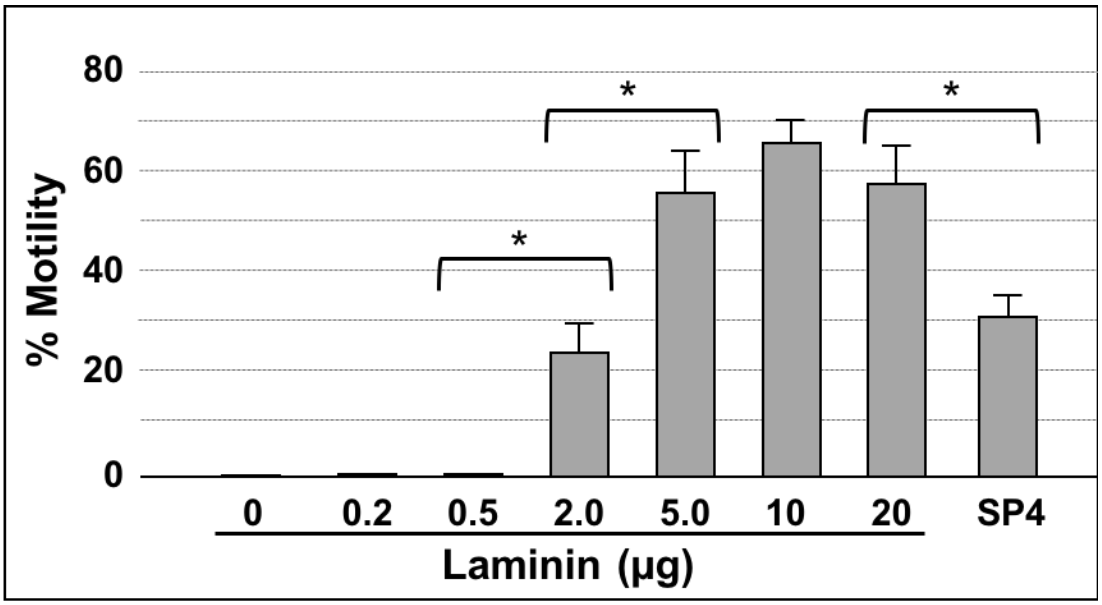
80
60
40
20
0
% Motility
*
*
*
0
0.2
0.5
2.0
5.0
10
20
SP4
Laminin (µg)

Figure 6. ***M. pneumonaie*** **gliding frequency on sialylated glycoproteins.** Gliding frequency for *M. pneumoniae* cells binding chamber slides coated with laminin at the indicated amounts. Each bar represents the mean and positive standard error of the mean for gliding frequency for three separate experiments. SP4, data for chamber slides coated with serum glycoproteins in SP4 growth medium, which served as a positive control. * P<0.001 for 2.0, 5.0, 10, and 20 μg laminin relative to lower laminin levels; ** $P < 0.001$ for 20 μg laminin relative to the SP4 control.

Table 1. *M. pneumoniae* gliding speeds on sialylated receptors. *M. pneumoniae* gliding speed on chamber slides coated with laminin or functionalized slides with α-2,3-sialyllactose.

Substrate	Gliding Speed[4,5]
Laminin[1]	0.34 μm/sec ± 0.113
α-2,3-sialyllactose[2]	0.28 μm/sec ± 0.234
SP4[3]	0.33 μm/sec ± 0.152

[1]Laminin concentrations were 2, 5, and 10 μg.

[2] α-2,3-sialyllactose 16, 32, and 80% were tested.

[3] Chamber slides coated with SP4 growth medium as positive control.

[4] Over 200 cells were tracked per substrate at each concentration across three separate experiments.

[5] No significant difference is seen between gliding speed with increase in concentration, gliding speed shown represents average range of all cells at all concentrations.

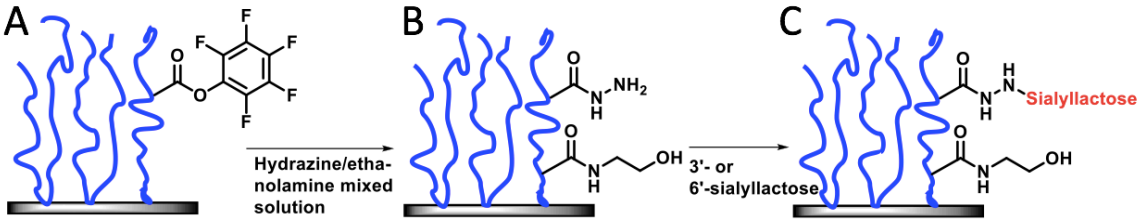
A
B
C
Hydrazine/etha-
nolamine mixed
solution
3'- or
6'-sialyllactose
Sialyllactose

Figure 7. **Schematic for surface conjugation.** Schematic representation of poly(PFPA) brushes (blue) conjugated to glass (A), with the subsequent conjugation of hydrazine at various ratios with competing ethanolamine (B) dictating the density of hydrazide available for (C) ligation with the reducing end of sialyllactose (red).

density of hydrazide available for ligating α-2,3- and α-2,6-sialyllactose to the poly(PFPA) scaffold (Fig. 7). In collaboration with Li Chen, Department of Chemistry, University of Georgia, we assessed the chemical modifications at each step by ellipsometry, drop shape analysis, and Fourier transform infrared spectroscopy for thickness, hydrophobicity and chemical changes of the thin polymer film, respectively (206)(data not shown). On average, ~10-nm hydrophilic glycosurfaces were built on ~15-nm thick poly(PFPA) hydrophobic films. In addition, surface analysis by atomic force microscopy demonstrated smooth and featureless topologies, with a root mean squared roughness of ~1 nm (data not shown). Table 2 shows the hydrazine/ethanolamine ratios we utilized, the resulting percentages of conjugation sites occupied by α-2,3-sialyllactose, and the corresponding estimated sialic acid density.

M. pneumoniae attachment and gliding on sialyllactose-functionalized surfaces

In collaboration with Li Chen, Department of Chemistry, University of Georgia, we conjugated α-2,3- or α-2,6-sialyllactose at the reducing ends to poly(PFPA) at densities ranging from 1.6% to 80%. *M. pneumoniae* attached to α-2,3-sialyllactose in a concentration-dependent manner. Attachment at α-2,3-sialyllactose densities of 16%, 32% and 80% were statistically comparable to that seen with the SP4 growth medium control, and binding saturation was evident at 16% α-2,3-sialyllactose (Fig. 8). Attachment to α-2,6-sialyllactose was significant but substantially lower than for α-2,3-sialyllactose and never achieved the levels observed for the SP4 control. We observed very minimal attachment ($\leq$ 10 cells per field) to the poly(PFPA) scaffold with 100% ethanolamine (i.e. no sialyllactose; data not shown). Treatment of α-2,3-sialyllactose and

Table 2. Sialyllactose conjugation density. Sialyllactose density conjugated to poly(PFPA) as a percentage of maximum possible at the indicated hydrazine: ethanolamine ratios.

Hydrazine/Ethanolamine	Actual resulting % hydrazide	Final % sialyllactose[1]	Calculated sialyllactose density (molecules/cm^2)[2]
1:999	2%	1.6%	5.4 x 10^{13}
1:199	10%	8%	2.7 x 10^{14}
1:99	20%	16%	5.4 x 10^{14}
1:39	40%	32%	1.1 x 10^{15}
100:0	100%	80%	2.7 x 10^{15}

[1]Conjugation of sialyllactose to hydrazide is 80% efficient, allowing for a maximum of 80% sialyllactose conjugate to a poly(PFPA)-grafted surface with hydrazide linkage.

[2]Density calculated using $d = \frac{A}{\varepsilon \cdot 1000} N_a$, where d is functional density in molecules/cm^2, A is absorbance, ε is the extinction coefficient of chromophore at λ_{max}, and N_a is Avogadro's number

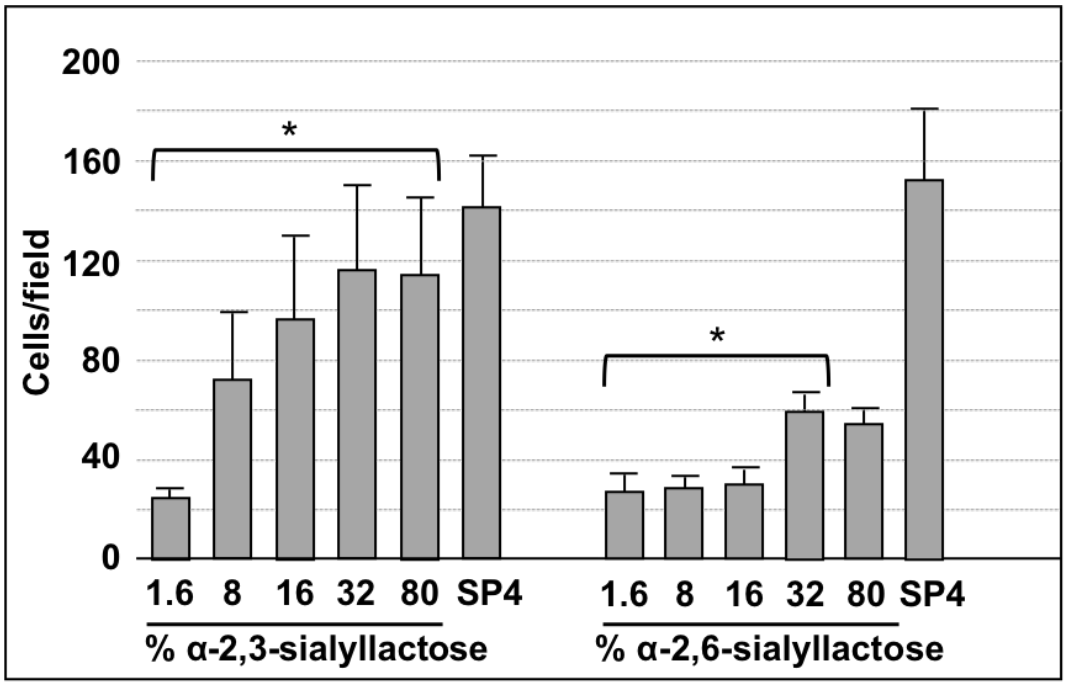
200
160
120
80
40
0
Cells/field
*
*
1.6
8
16
32
80
SP4
1.6
8
16
32
80
SP4
% α-2,3-sialyllactose
% α-2,6-sialyllactose

Figure 8. *M. pneumoniae* attachment on sialyllactose. *M. pneumoniae* attachment to slides chemically functionalized with α-2,3- or α-2,6-sialyllactose, as indicated. Each bar represents the mean and positive standard error of the mean for total cell counts at a given sialyllactose percentage for three separate experiments. SP4, chamber slides coated with SP4 growth medium as a positive control. * $P < 0.001$ for cell numbers on 1.6% α-2,3-sialyllactose relative to the higher α-2,3-sialyllactose percentages; ** $P < 0.001$ for cell numbers on 32% and 80% α-2,6-sialyllactose relative to the lower α-2,6-sialyllactose percentages; *** $P < 0.001$ for cell numbers on SP4 relative to all percentages of α-2,6-sialyllactose.

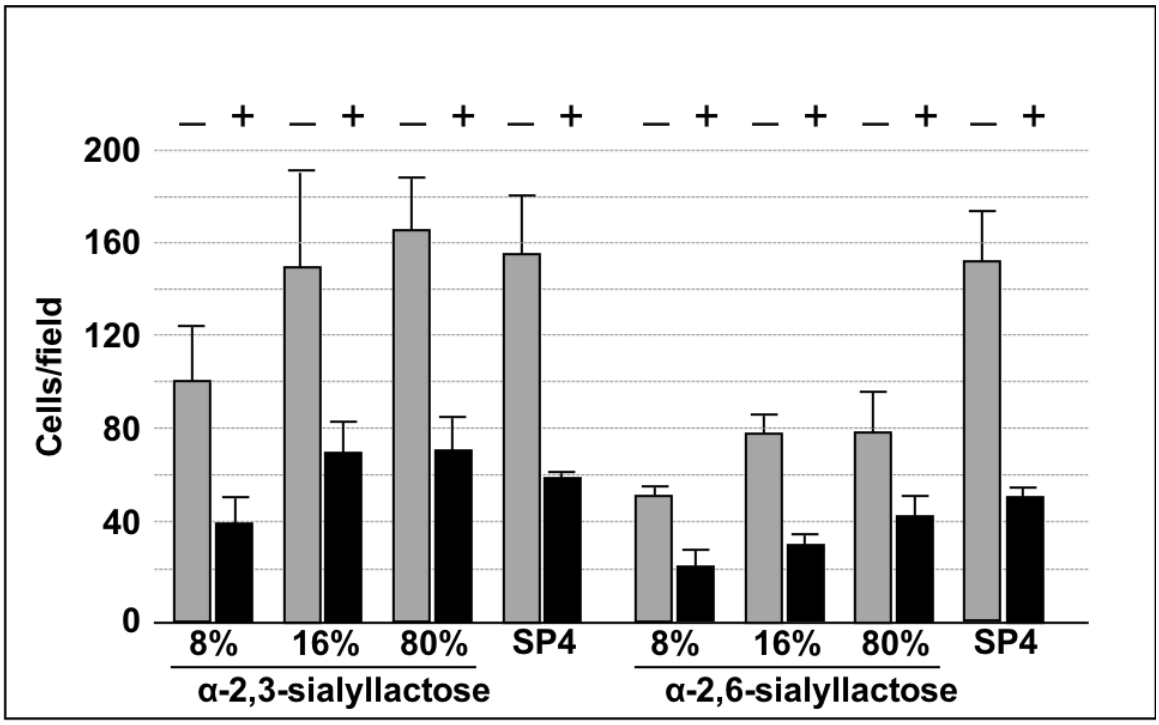
– + – + – + – + – + – + – + – +
200
160
120
80
40
0
Cells/field
8%
16%
80%
SP4
8%
16%
80%
SP4
α-2,3-sialyllactose
α-2,6-sialyllactose

Figure 9. **Effect of neuraminidase treatment of sialyllactose surfaces on attachment.** *M. pneumoniae* attachment to slides functionalized with sialyllactose with and without pre-treatment with neuraminidase. Each bar represents the mean and positive standard error of the mean for attached cells for three separate experiments. SP4, data for chamber slides coated with serum glycoproteins in SP4 growth medium, which served as a positive control. + indicates neuraminidase pre-treatment ($P < 0.001$).

α-2,6-sialyllactose with neuraminidase resulted in significantly decreased attachment, confirming specificity for the sialic acid (Fig. 9). I observed no gliding on surfaces with a α-2,3-sialyllactose conjugation density lower than 8%, despite significant levels of attachment (Fig. 10). Gliding was prominent on α-2,3-sialyllactose at densities of 8% and higher. Gliding frequency increased between conjugation densities of 8% and 32% but then decreased at higher conjugation densities. No gliding was observed on surfaces conjugated with α-2,6-sialyllactose at any concentration or on α-2,3-sialyllactose following pre-treatment with neuraminidase. Gliding speed was consistently 0.26-0.28 μm/sec for all α-2,3-sialyllactose concentrations that supported gliding (Table 1).

In order to investigate whether α-2,6-sialyllactose influences gliding on α-2,3-sialyllactose, we conjugated both oligosaccharides to poly(PFPA) at different ratios (Table 3). We also prepared poly(PFPA) surfaces in parallel with competing ethanolamine, in the manner described in Table 2, to allow direct comparison on an equivalent amount of α-2,3-sialyllactose alone (Fig. 11). In each case, the presence of α-2,6-sialyllactose with α-2,3-sialyllactose reduced the gliding frequency below what was observed on the same amount of α-2,3-sialyllactose alone (Table 3).

M. pneumoniae binding and gliding on a sulfated glycolipid

Previous studies (14) established that *M. pneumoniae* binds to sulfatide in a concentration-dependent manner. However, gilding motility by sulfatide-bound mycoplasmas has not been explored. We began by confirming *M. pneumoniae* binding to sulfatide to establish a baseline for subsequent gliding analysis. *M. pneumoniae* bound to chamber slides coated with sulfatide in a concentration dependent-manner, as expected (14), with saturation at 5μg (Fig. 12). At the highest concentrations tested, attachment

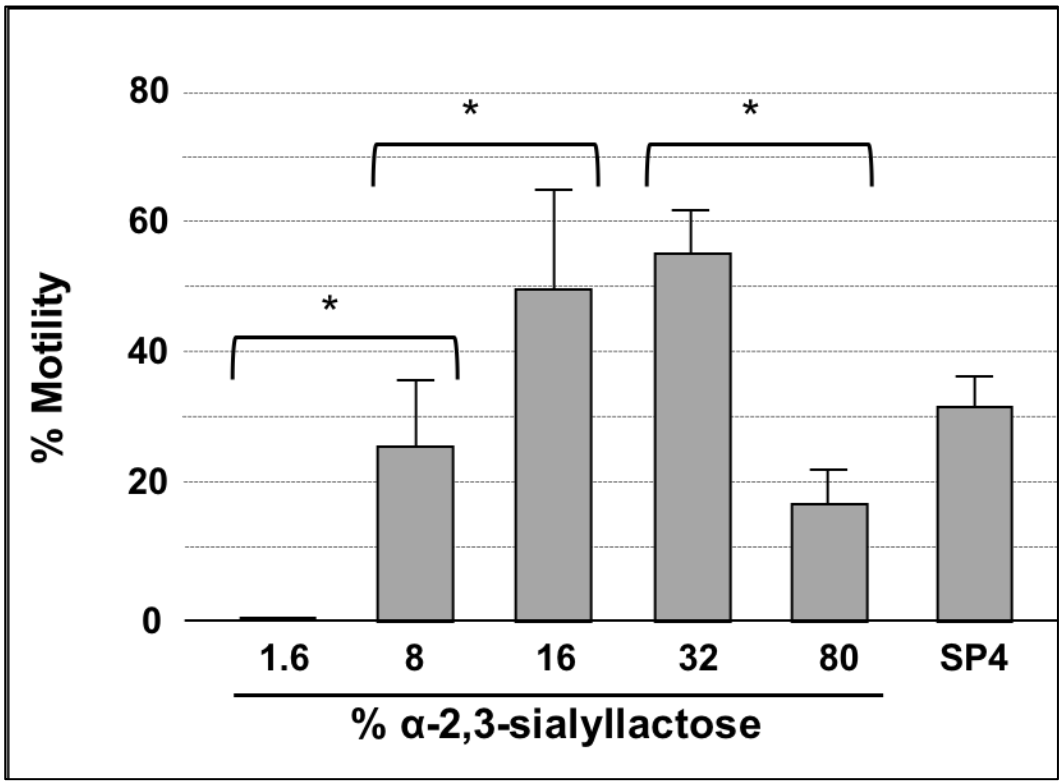

levels were comparable to chamber slides pre-treated with SP4 growth medium (Fig. 12).

Addition of dextran

Figure 10. ***M. pneumoniae*** **gliding frequency on α-2,3 sialyllactose**. Gliding frequency for *M. pneumoniae* cells attached to slides chemically functionalized with α-2,3 sialyllactose. Each bar represents the mean and positive standard error of the mean for gliding frequency for three separate experiments. SP4, data for chamber slides coated with serum glycoproteins in SP4 growth medium, which served as a positive control. *P=<0.001.

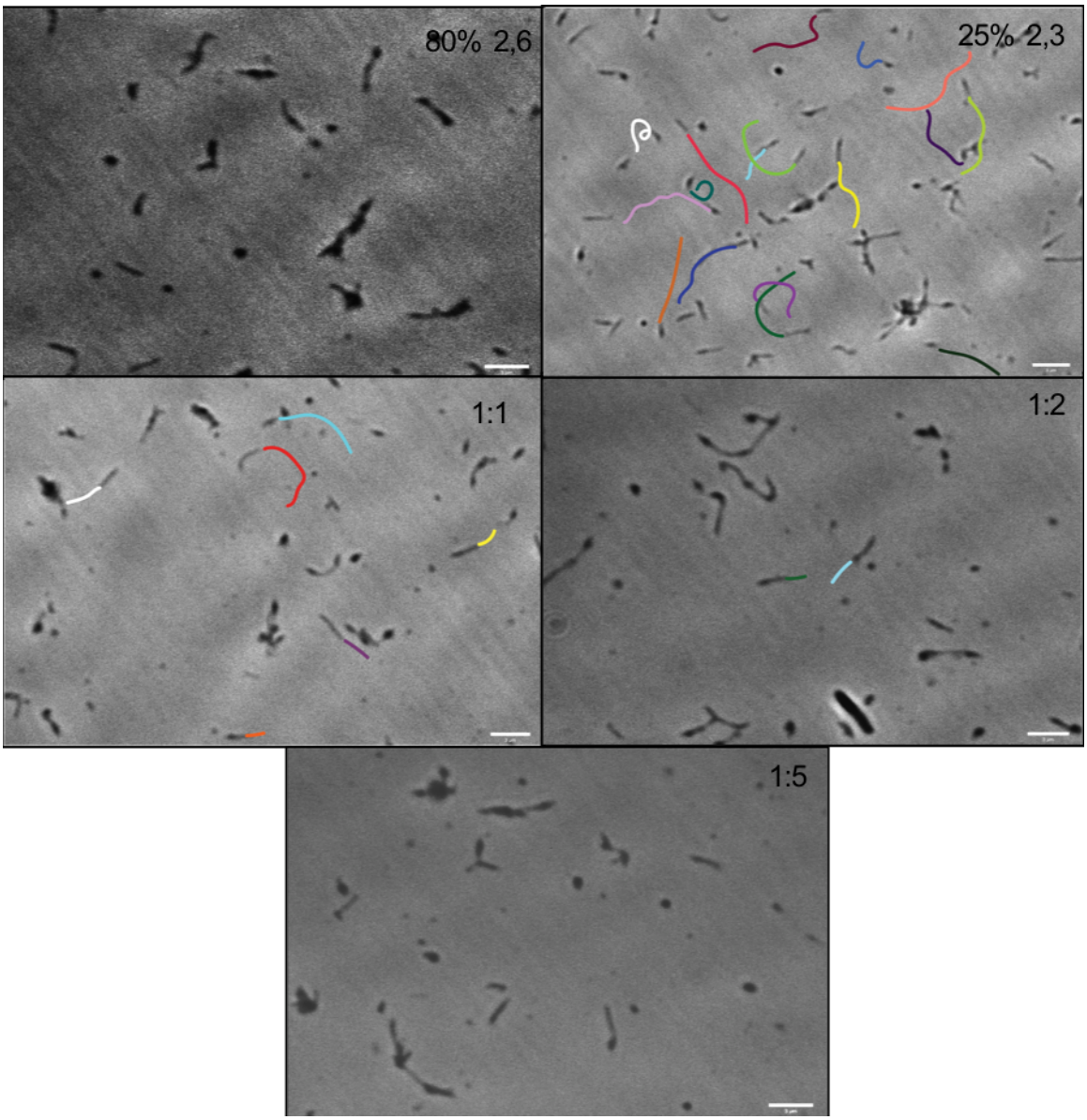
80% 2,6
25% 2,3
1:1
1:2
1:5

Figure 11. *M. pneumoniae* gliding tracked on α-2,3 and α-2,6 surfaces. Phase images of live *M. pneumoniae* on functionalized surfaces with α-2,3-sialyllactose : α-2,6-sialyllactose ratios of 1:2 and 1:5, as well as α-2,3-sialyllactose at 25% and α-2,6-sialyllactose at 80%. Colored lines indicate gliding tracks of individual cells, cells are tracked for 20 consecutive images over 40 seconds.

Table 3. *M. pneumoniae* attachment and gliding on α-2,3 and α-2,6 surfaces in combination. *M. pneumoniae* gliding motility on surfaces having α-2,3-sialyllactose and α-2,3-sialyllactose conjugated at the indicated ratios.

Ratio of α-2,3- : α-2,6-sialyllactose for conjugation	Resulting α-2,3- : α-2,6-sialyllactose on surface (%)	Cells per Field[2]	Motility (%)[3]
NA[1]	27:0	178.735.6	63%
1 : 1	27:27	116.7±20.6	10%
1 : 2	27:53	92.7±13.1	6%
NA	14:0	121±22.5	17%
1 : 5	13:67	82.3±10.8	1%
0 : 100	0:80	62.9±7.4	0%

[1] NA, not applicable; amount of α-2,3 sialyllactose conjugated was controlled by varying the hydrazine/ethanolamine ratio, as in Table 1, rather that its ratio to α-2,6-sialyllactose

[2] $P < 0.001$ for difference between 27:0 and 27:27 or 27:53, $P < 0.03$ for difference between 14:0 and 14:66

[3] $P < 0.001$ for differences between 27:0 and 27:27 or 27:53; $P < 0.05$ for difference between 14:0 and 14:66

sulfate, a competitive binding inhibitor to sulfatide, to the *M. pneumoniae* culture resulted in a 50-55% reduction in *M. pneumoniae* attachment, ($P<0.002$), consistent with a binding specificity for sulfated moieties, as expected (Fig. 13) (14). We also examined binding of *M. pneumoniae* to sulfatide-coated chamber slides at 4°C or 37°C. Incubations at 4°C resulted in a 60-95% reduction in *M. pneumoniae* attachment across the varying concentrations tested compared to incubations at 37°C ($P<0.001$) (Fig. 14). Finally, we analyzed gliding motility of *M. pneumoniae* bound to sulfatide. In contrast to the gliding observed on laminin (Fig. 15B) and the SP4 control (data not shown), mycoplasmas bound to sulfatide were non-motile at all sulfatide levels tested (Fig. 15A and data not shown).

M. pneumoniae binding of terminal organelle mutants on glycan receptors

Previous studies have described an assortment of *M. pneumoniae* mutants exhibiting a range of defects in terminal organelle function. Of particular interest to us were two mutants in the P30 protein, which localizes to the distal end of the terminal organelle (Fig. 1) and is essential for the adhesin P1 to be fully functional (reference). The II-3 mutant lacks P30 due to a frameshift at position 453 in MPN453, loss of P30 results in an altered cell morphology, no cytadherence, and no gliding motility (3). The revertant II-3R has a second-site mutation that restores the wild-type reading frame for all but 17 residues (3). II-3R attaches to erythrocytes at wildtype levels, but has a reduced gliding frequency and gliding speed (126). We examined wildtype *M. pneumoniae,* the P30 mutant II-3, and the revertant II-3R for binding to laminin and sulfatide-coated chamber slides, and to α-2,3-sialyllactose. Binding by the II-3 mutant was 4% of wildtype levels on laminin and α-2,3-sialyllactose, as expected, based on its

hemadsorption-negative phenotype (Fig. 16A) (8). In contrast, and somewhat unexpectedly, the II-3 mutant bound to sulfatide at 58% of wild-type levels (Fig. 16A). Furthermore, binding by the II-3R revertant was comparable to wildtype on sulfatide and the positive control of SP4 growth medium, as expected, but only 35% of wildtype levels on laminin (Fig 16B) (126, 209).

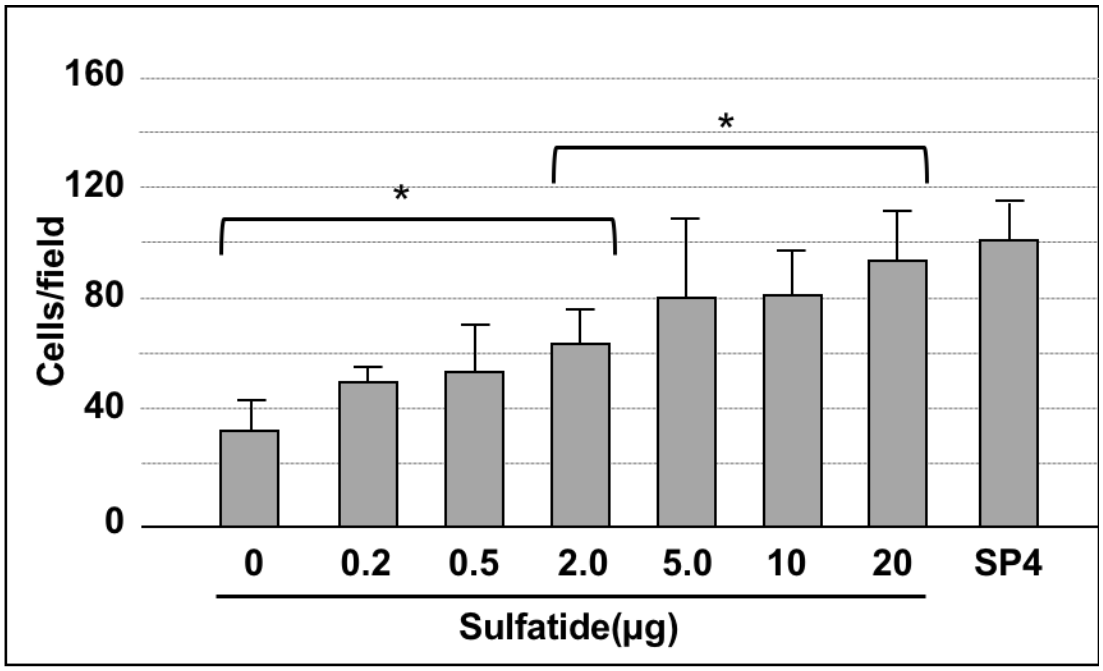
160
120
80
40
0
Cells/field
*
*
0
0.2
0.5
2.0
5.0
10
20
SP4
Sulfatide(μg)

Figure 12. *M. pneumoniae* attachment to a sulfated glycolipid. *M. pneumoniae* attachment to chamber slides coated with sulfatide at the indicated levels. Each bar represents the mean and positive standard error of the mean for total cell counts for three separate experiments. SP4, data for chamber slides coated with serum glycoproteins in SP4 growth medium, which served as a positive control. *$P < 0.001$ for 2.0, 5.0, 10, and 20 µg sulfatide relative to the 0µg control. **P<0.001 for 2µg relative to 20µg.

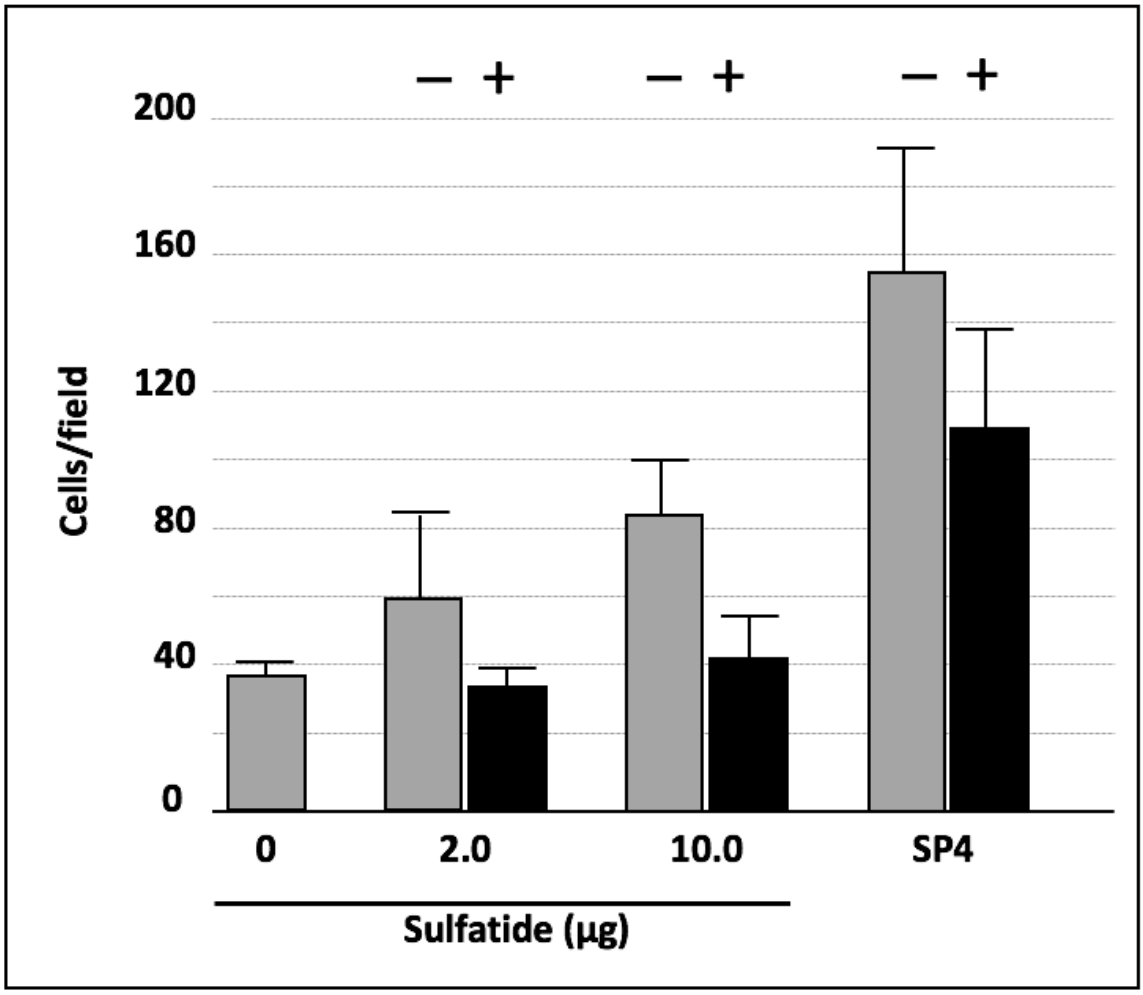
− +
− +
− +
200
160
120
80
40
0
Cells/field
0
2.0
10.0
SP4
Sulfatide (µg)

Figure 13. Inhibition of attachment to sulfatide coated surfaces by dextran sulfate. *M. pneumoniae* attachment to chamber slides coated with sulfatide, with and without competing dextran sulfate. Each bar represents the mean and positive standard error of the mean for attached cells for three separate experiments. SP4, data for chamber slides coated with serum glycoproteins in SP4 growth medium, which served as a positive control. + indicates addition of dextran sulfate. $P < 0.001$ when comparing + dextran sulfate at all concentrations.

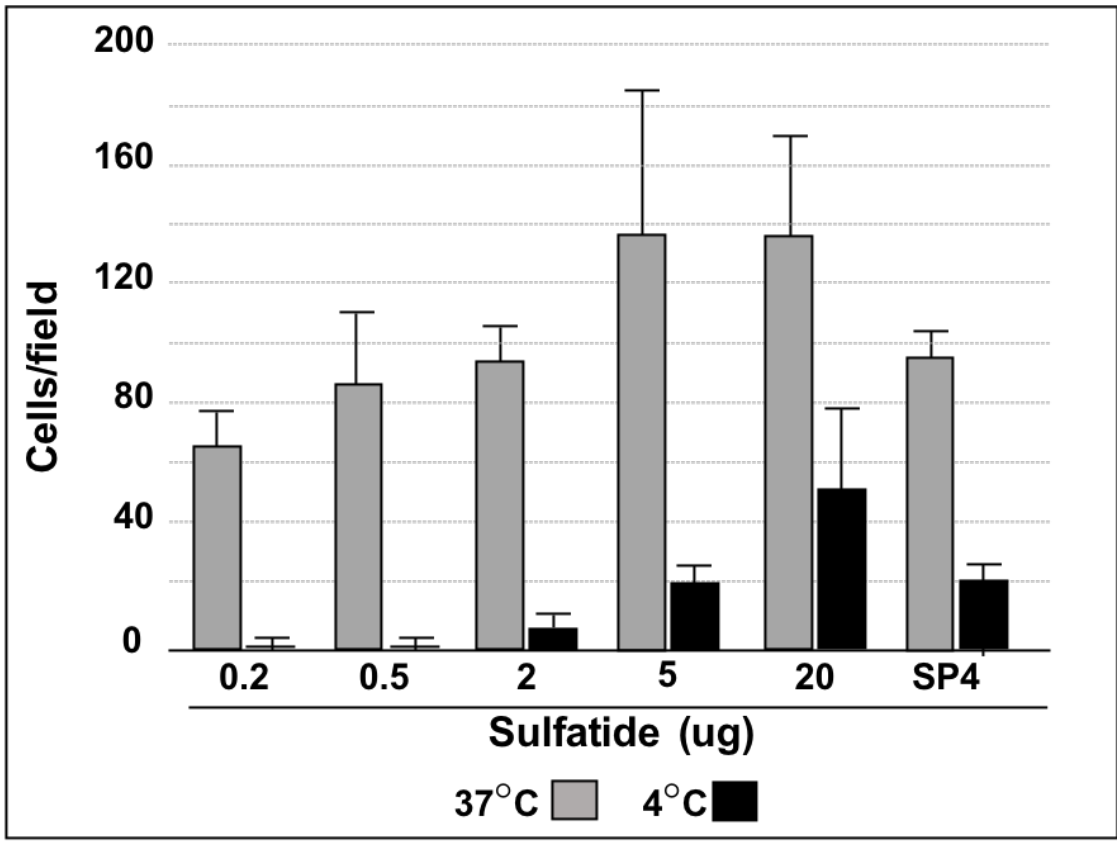
200
160
120
80
40
0
Cells/field
0.2
0.5
2
5
20
SP4
Sulfatide (ug)
37°C
4°C

Figure 14. Effect of temperature on attachment to sulfated glycolipids. *M. pneumoniae* attachment to chamber slides coated with sulfatide, with incubations at 37°C or 4°C. Each bar represents the mean and positive standard error of the mean for attached cells for three separate experiments. SP4, data for chamber slides coated with serum glycoproteins in SP4 growth medium, which served as a positive control. $P < 0.001$ between 37°C and 4°C for each concentration.

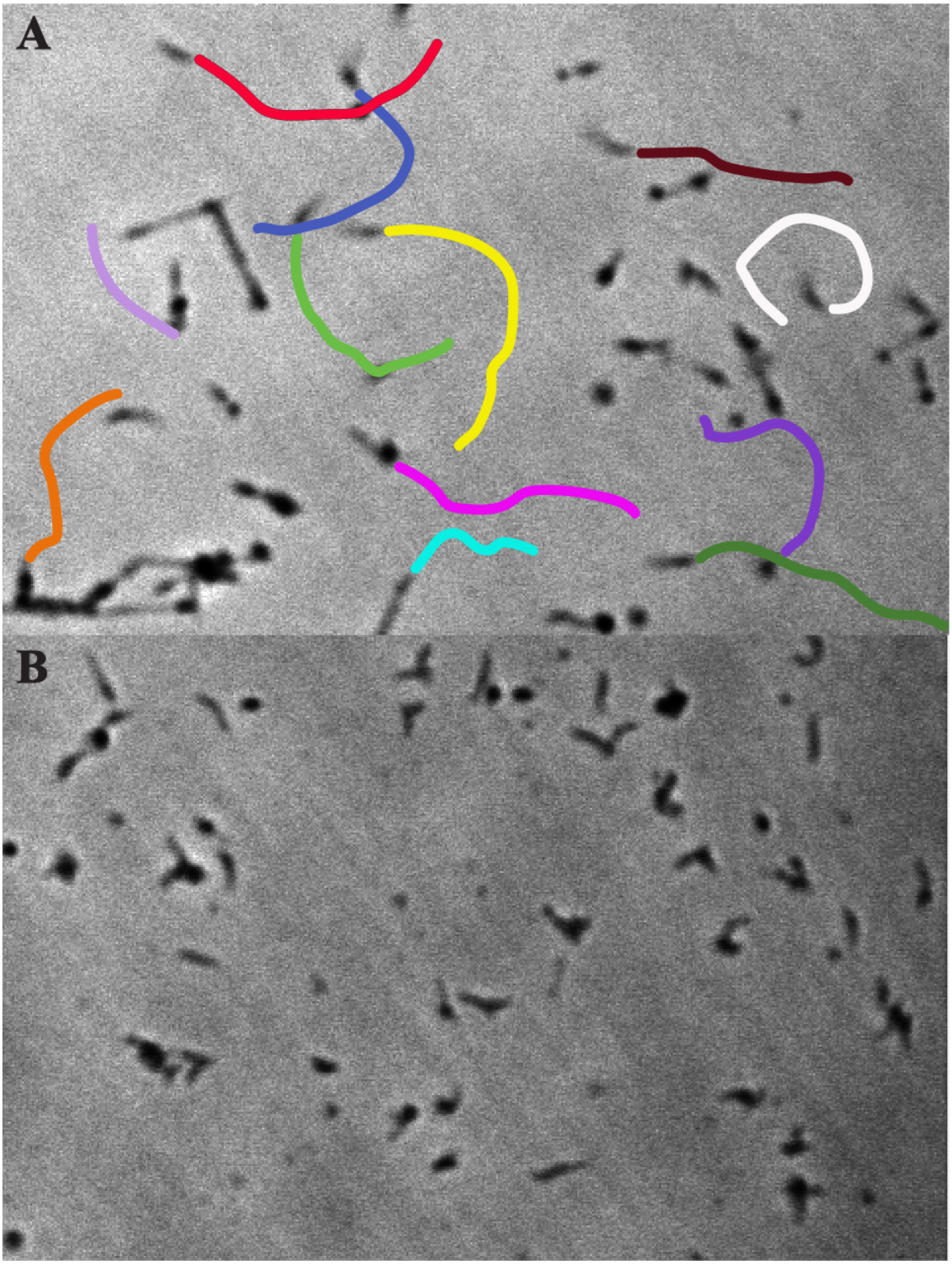
A
B

Figure 15. *M. pneumoniae* gliding tracked on sialylated and sulfated receptors.

Phase contrast images of live *M. pneumoniae* on glass chamber slides coated with 20ug of (**A**) laminin or (**B**) sulfatide. Colored lines indicate gliding tracks of individual cells. Cells were tracked for 20 consecutive images over 40 seconds.

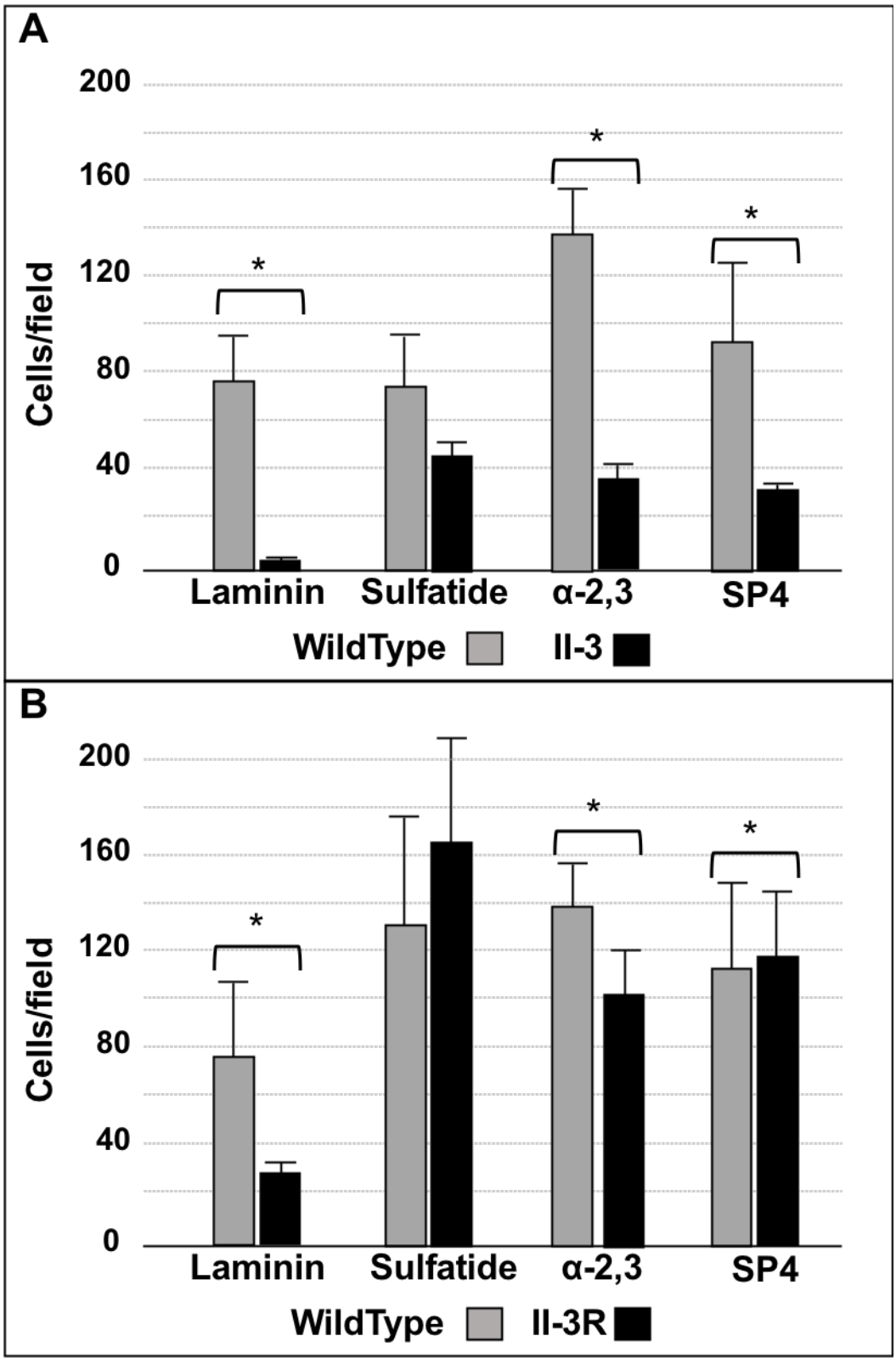
A
200
160
120
80
40
0
Cells/field
*
*
*
Laminin
Sulfatide
α-2,3
SP4
WildType
Il-3
B
200
160
120
80
40
0
Cells/field
*
*
*
Laminin
Sulfatide
α-2,3
SP4
WildType
Il-3R

Figure 16. *M. pneumoniae* P30 mutant attachment on glycan receptors. Attachment by wildtype *M. pneumoniae* and P30 mutant II-3 (**A**) or P30 revertant II-3R (**B**) to chamber slides coated with sulfatide or laminin at 10μg, and slides functionalized with α-2,3 sialyllactose at 32%. Each bar represents the mean and positive standard error of the mean for attached cells for three separate experiments. $*P < 0.001$

CHAPTER 5

DISCUSSION

Modeling interaction of *M. pneumoniae* and sialylated receptors

Glycoprotein receptors having terminal sialic acid residues are fundamentally important in *M. pneumoniae* binding to human airway epithelium, and *in vitro* proxies thereof (16, 210). Moreover, this requirement for sialic acid recognition encompasses subsequent mycoplasma gliding motility on inert surfaces (17), and likely on epithelial surfaces, although this has only been suggested indirectly (10, 128). Mycoplasma gliding requires repeated binding and release of receptors in order to allow movement across a surface (129, 179, 211), reflecting the dynamic nature of this bacterial ligand / host receptor interaction. *M. pneumoniae* exhibits higher binding affinities in suspension for sialic acids having α-2,3 linkages over those linked α-2,6 (17), but the nature of surface-bound receptor recognition in *M. pneumoniae* adherence and gliding activity are otherwise poorly understood and likely influenced by local receptor environment. Here I utilized glass surfaces either coated by physisorption with sialylated glycoproteins, or precisely conjugated with sialyl-oligosaccharides via an inert scaffold, to begin to examine the influence of receptor environment on *M. pneumoniae* attachment and gliding. I observed concentration-dependent and sialic acid-specific attachment of *M. pneumoniae* to both the more heavily sialylated glycoprotein laminin, and the less sialylated glycoprotein hCG, consistent with previous studies (15). Laminin supported mycoplasma attachment at levels that were comparable to that for serum glycoproteins in

SP4 growth medium and significantly greater than that for hCG (Fig. 7). While laminin at concentrations of 2 μg and higher supported *M. pneumoniae* gliding motility (Fig. 6), *M. pneumoniae* was non-motile on laminin at lower concentrations, and on hCG at any concentration, despite the significant levels of attachment observed (Fig. 7). Thus, a sialic acid receptor density threshold is required for the initiation of gliding, and that threshold is greater than the receptor density necessary to support mycoplasma attachment. Mycoplasma gliding frequency correlated with receptor density, increasing with higher concentrations of laminin. In contrast, gliding speed remained consistent for all laminin concentrations tested.

Glycoproteins adsorbed to an inert surface provide a convenient and informative model for studying *M. pneumoniae* – host receptor interactions. However, this approach has significant limitations, most notably that the amount of glycoprotein bound to the glass surface, and thus the actual density of sialic acid residues, is poorly defined. Moreover, glycosylation of the substrate protein is subject to variability, with no control over carbohydrates linkages, composition, or arrangement (e.g. linear vs. branched). This prompted us to pursue an approach that overcomes these limitations and yields functionalized surfaces with more precisely defined oligosaccharide presentations. Our initial attempt involved poly(PFPA)-grafted surfaces that were conjugated with polyethylene glycol (PEG) followed by the sialylated glycoprotein fetuin. However, working with the large protein made functionalization difficult without denaturing the protein. This led to the pursuit of simple oligosaccharides, starting with α-2,3-sialyllactose. Due to non-specific attachment of *M. pneumoniae* cells to PEG, we began to work with hydrazine as a linker between the poly(PFPA) and the sugar. We were able

to determine that *M. pneumoniae* attachment to hydrazine was negligible, so any remaining hydrazide linkages would not interfere with *M. pneumoniae* attachment studies. Conjugation of α-2,3- sialyllactose to poly(PFPA)-grafted surfaces through a hydrazide linkage was successful and confirmed to be functional by staining with the sialic-acid binding lectin wheat germ agglutinin (WGA) (206). To this end we recently described the successful methodology for this ligation of oligosaccharides at the reducing end to poly(PFPA)-grafted surfaces through a hydrazide linkage (206). Next, we expanded upon that approach, varying the density of hydrazide linkages available by changing the ratios of hydrazine and competing ethanolamine in the conjugation to poly(PFPA) (Fig. 7), making it possible to control the density of α-2,3- or α-2,6-sialyllactose precisely in the subsequent ligation to hydrazide.

Both α-2,3- and α-2,6-sialyllactose supported *M. pneumoniae* attachment in a concentration-dependent manner. However, mycoplasma binding to α-2,6-sialyllactose never achieved the levels observed with α-2,3-sialyllactose or the SP4 control. This is consistent with both the lower binding affinity reported for *M. pneumoniae* and α-2,6-sialyllactose in suspension (17), and the higher levels of α-2,6-sialyllactose required to inhibit *M. pneumoniae* attachment to laminin (15). Neuraminidase pre-treatment of surfaces conjugated with α-2,3- or α-2,6-sialyllactose resulted in significantly decreased mycoplasma attachment (Fig. 9). Increasing the amount of neuraminidase or treatment time did not reduce attachment levels further (data not shown). The residual mycoplasma attachment to neuraminidase-treated sialyllactose probably reflects mycoplasma binding to the remaining lactose after removal of the sialic acid residues, based upon the previous

observation by Krivan et al. (14) of low levels of *M. pneumoniae* binding to lactosylceramide.

Only α-2,3-sialyllactose supported *M. pneumoniae* gliding motility (Fig. 10), and as noted above with laminin, a threshold density of α-2,3-sialyllactose existed, below which mycoplasma attachment was evident but not gliding motility. These results are consistent with the two-step model of gliding motility for *M. pneumoniae* (129), where the "catch" and "release" interaction between the P1 adhesin complex and sialyl receptors occurs repeatedly during gliding. The P1 adhesin complex is able to engage both α-2,3- and α-2,6- sialyl receptors, as evidenced by the ability of either in solution to competitively inhibit receptor binding by gliding *M. pneumoniae*, resulting in their detachment from the surface (17), and by our attachment data here (Fig. 5 and 6). However, sialic acids linked α-2,3 but not α-2,6 may trigger a secondary recognition event, such as a conformational change in the adhesin complex, resulting in the "catch" that engages the now bound adhesin complex in treadmilling, and allows initiation of gliding. *M. pneumoniae* attachment may be similar in this respect to the initial and tight, two-step binding described for gliding by *Mycoplasma mobile* (179). If sialic acid linked α-2,3 is too sparse, insufficient P1 adhesin complexes engage to drive *M. pneumoniae* cell movement and gliding motility. Here no gliding occurred on chemically functionalized surfaces having α-2,3-sialyllactose densities below an estimated 0.54 residues per nm^2. It should be noted that the poly(PFPA) matrix extends into three-dimensional space, but we did not attempt to consider depth in our sialyllactose density estimate for two reasons. First, thickness measurements were recorded for dehydrated films, and the depth of the hydrated matrix will vary with extent of conjugation. Second,

the average conjugation efficiency with different oligosaccharides may vary from 80% to 90%, and it is not known if conjugation is uniform throughout the depth of the film or may reflect steric inhibition within the matrix.

Mycoplasma gliding frequency increased with α-2,3-sialyllactose density, but only to a point. At the highest α-2,3-sialyllactose densities tested, *M. pneumoniae* gliding frequency decreased relative to maximum gliding frequencies observed at lower sialyllactose densities. This reduction might reflect an issue with avidity, where too many adhesin complexes are engaged and therefore unavailable to sustain cell movement via treadmilling. In contrast, gliding speed did not change with receptor density, both with laminin and α-2,3-sialyllactose, and in this respect *M. pneumoniae* gliding behavior differed from that described for *M. mobile,* where gliding speed varies with sialyllactose density (179). This may be due to the difference in proposed gliding mechanism, where *M. mobile* utilizes a centipede model where the power for the mechanism comes from the "leg" proteins (132). While, *M. pneumoniae* utilizes a treadmilling model where the power for the mechanism may come from the electron-dense core. It is possible that the difference in the gliding mechanism may not allow for *M. pneumoniae* to increase gliding speed despite higher densities of receptors.

Differential lectin histochemistry studies indicate that sialic acids (linked both α-2,3 and α-2,6) are expressed on the surface of normal human bronchial epithelial cells that differentiated *in vitro* (212). However, the relative distribution of each linkage type reportedly varies in different regions of intact airways, again based upon lectin histochemistry (178). In all cases, it is clear that the airway mucosa presents a heterogeneous array of sialylated and other oligosaccharides, with *M. pneumoniae* likely

to encounter sialic acids in diverse linkages and relative abundances. In order to begin to explore how this diversity might affect *M. pneumoniae* gliding behavior we conjugated α-2,3 sialyllactose and α-2,6 sialyllactose to poly(PFPA) at varying ratios. Our results consistently revealed reduced gliding on α-2,3 sialyllactose when conjugated in combination with α-2,6 sialyllactose. We believe that the simplest interpretation of this inhibition is competition by α-2,6 sialyllactose for binding by P1 adhesin complexes. As α-2,6 sialyllactose fails to support gliding, this competitive inhibition could limit the number of P1 adhesin complexes engaged with α-2,3 sialyllactose and therefore could contribute to cell gliding. This interplay between P1 adhesin complexes and sialic acids with diverse linkages and presentations on airway epithelium could potentially have a major impact on mycoplasma localization and mobilization in different regions of the conducting airways, depending on the relative abundance of α-2,6 sialyl linkages.

Modeling *M. pneumoniae* interactions with sulfated receptors

M. pneumoniae has been previously shown to bind to sulfated glycolipids, with a specificity for binding Gal($3SO_4$)ß1 residues (14). Compared to sialylated receptors, much less is known regarding *M. pneumoniae* interactions with sulfated receptors. Current understanding is largely limited to the potential for sulfatide to support *M. pneumoniae* attachment (14). Here I confirmed and expanded upon previous work to examine *M. pneumoniae* attachment and gliding motility on the sulfated glycolipid sulfatide. I utilized glass surfaces coated by physisorption with sulfatide at varying concentrations, observing concentration-dependent and sulfate-specific attachment of *M. pneumoniae* to sulfatide, consistent with previous studies (14). At the highest concentrations, sulfatide attachment levels were comparable to the SP4 positive control

(Fig. 12). The biological relevance for sulfatide adhesion is strengthened by the necessity for *M. pneumoniae* cells to be metabolically active to attach, indicated by decreased attachment at 4°C, consistent with previous studies (144, 185, 213). Sulfatide is also found in high amounts in the human trachea making it physiologically relevant as a potential *M. pneumoniae* receptor (14).

Unlike the sialylated glycoprotein laminin, sulfatide did not promote *M. pneumoniae* gliding motility at any concentration tested (Fig. 15B). It is not clear why sulfatide does not promote gliding motility despite supporting high levels of attachment. It is possible that sulfate binding involves a different adhesin than the P1 adhesin complex that binds α-2,3 sialyl linkages, leading to cell gilding; the putative sulfated glycan adhesin may not engage the gliding mechanism. Alternatively, the sulfate moieties may bind with the adhesin complex, but with a high binding affinity that prevents the "catch" and "release" mechanism necessary for gliding motility to occur. To better understand the possible adhesin that binds sulfatide we will conduct studies using a P1-specific monoclonal antibody that is known to disrupt sialic acid binding. If this monoclonal antibody also prevents attachment to sulfatide, this would suggest that P1 plays a direct role in recognition and attachment to sulfatide. Conversely, failure of the monoclonal antibody to block binding to sulfatide would suggest an alternative adhesin. Furthermore, atomic force microscopy studies currently in progress and described below should reveal binding force to sulfated and sialylated receptors and may elucidate further the nature of the sulfatide adhesin.

While the glycolipid adsorbed to an inert surface allows for a simple model for studying *M. pneumoniae*-host receptor interactions, it has similar limitations to the

glycoprotein studies above. To create a more precisely defined surface we will utilize functionalized surfaces that allow for better defined oligosaccharide presentation, similar to the α-2,3- and α-2,6-sialyllactose studies. However, these studies will require a modified chemistry for functionalization of a sulfated sugar to the surface. Initial attempts to ligate sulfated oligosaccharides through hydrazine conjugation proved to be inefficient due to the chemical charge of the sulfate moiety. With the help of the Gert-Jan Boons lab we have been able to identify an alternative strategy to conjugate sulfated oligosaccharides directly to poly(PFPA)-grafted surfaces. This change in chemistry does result in a lower ligation efficiency compared to hydrazine, with a decrease from 80% with hydrazine to 60-70%. We will test surfaces functionalized with sulfated sugars at varying concentrations in the near future. This modified chemistry will also support future studies with sulfated sugars and sialyllactose ligated to poly(PFPA) in combination to observe gliding behavior in the presence of both receptors.

M. pneumoniae terminal organelle mutant interactions with glycan receptors

There are a large number of terminal organelle mutants available for *M. pneumoniae*, some having extreme changes in phenotype, while others having more subtle changes (5, 7, 96, 102, 110, 111, 139). These mutant strains are an important resource for studying terminal organelle function and have shed light on the mechanism of attachment and gliding motility (122, 100). In the current studies, we utilized two terminal organelle mutants of the P30 protein. The P30 mutant II-3 has a frameshift mutation due to the loss of a single adenine nucleotide in the MPN453 ORF encoding P30 that leads to a lack of detectable P30 (Fig. 2)(3). Loss of P30 results in altered cell morphology, decreased cytadherence, and non-motility (3, 113, 126). The II-3 revertant

II-3R, derived from II-3, has a second frameshift mutation that restores the reading frame for all but 17 residues of the MPN453 reading frame (3). While this altered P30 (P30R) restores cytadherence and gliding motility, gliding frequency and speed are greatly reduced compared to wild-type levels (126). This suggests that while the II-3R revertant is able to attach, which is a prerequisite for gliding, there is a defect in the gliding mechanism due to the 17-residue amino acid substitution (126).

We examined adherence and gliding of mutant II-3 and revertant II-3R on surfaces coated with laminin and sulfatide or functionalized with α-2,3-sialyllactose. The II-3 mutant exhibited minimal attachment to laminin, α-2,3-siallylactose, and the SP4 positive control as expected (126). However, attachment of the II-3 mutant to sulfatide was comparable to wild-type levels (Fig. 15A). The II-3R revertant likewise attached to sulfatide and SP4 control wells at wild-type levels, but attached to laminin and α-2,3-sialyllactose at levels below wild-type (Fig. 15B). Unlike wild-type P30, P30R forms multimers that are unable to dissociate efficiently into monomers. This indicates that there may be a need for P30, with the ability to undergo proper conformational changes from multimers to monomers, to allow for *M. pneumoniae* recognition and attachment to sialic acid receptors but not necessarily to sulfated receptors. Electron cryotomography studies have revealed the presence of protein knobs on the terminal organelle surface that correspond to P1 adhesin complexes, and the density of these protein knobs on the terminal organelle from cell to cell can vary (146). Furthermore, these knobs are sparse on the II-3 mutant surface. It is possible that revertant II-3R may likewise have fewer knobs on the terminal organelle surface (3). The lack of functional P1 in II-3 also suggests that an alternate adhesin may direct attachment to sulfatide; this alternate

adhesin may be a different protein or a glycolipid on the cell surface, possibly located throughout the cell surface as opposed to localizing at the terminal organelle. We favor a model in which P30R multimers do not yield functional P1 adhesin complexes as readily as wild-type P30. This leads to a failure to adhere to sialylated residues, and generate motility comparable to wild-type levels, while an alternate adhesin is involved in attachment to sulfated receptors.

Studies on various terminal organelle mutants has shown the importance of attachment and gliding when *M. pneumoniae* cells infect the host (5, 6, 214). The II-3 mutant is unable to successfully colonize in animal models but it does attach to cell culture models at low levels (6, 10). Successful attachment to cell culture models may reflect sulfatide binding. Furthermore, sulfatide binding alone may not be sufficient for colonization of animal models, possibly due to the inability to interact with sialylated receptors necessary to initiate gliding motility. Interestingly, the P30 revertant II-3R was unable to infect BALB/c mice or colonize NHBE cells (6, 10) but can successfully adhere to hamster tracheal rings and colonize hamsters (215). It is possible that the difference in adherence seen in the revertant II-3R mutant could be due to the variation in nature and density of glycan receptors present in each model.

Elucidating *M. pneumoniae* binding force and adhesin location by atomic force microscopy

The studies above have allowed us to elucidate the nuances of *M. pneumoniae* attachment and gliding motility on sialylated and sulfated receptors, showing a distinct difference in gliding phenotype and attachment levels based on the nature and density of the receptor. However, these studies have left two important questions unanswered about

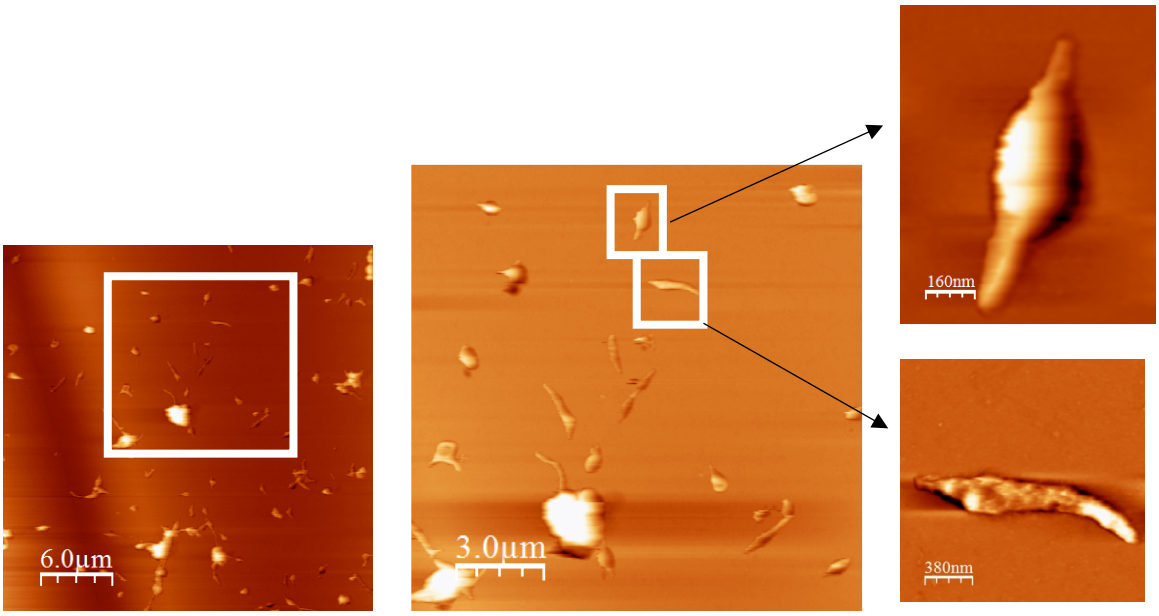
6.0µm
3.0µm
160nm
380nm

Figure 17. Fixed *M. pneumoniae* cells scanned by atomic force microscopy. Atomic force microscopy scans of fixed *M. pneumoniae* cells.

the interactions of *M. pneumoniae* and its receptors. First, what is the binding force between *M. pneumoniae* adhesin complexes and the receptor? Second, where on the cell surface do these interactions occur? It is possible that interactions may occur exclusively at the terminal organelle, which would be expected for P1 adhesin complexes, or along the entire length of the cell, which could suggest the use of alternative adhesins. These questions will be answered by utilizing atomic force microscopy (AFM) to measure binding force and map interaction of glycan receptors with live *M. pneumoniae* cells. In our preliminary work with the Bingqian Xu lab we have visualized chemically fixed *M. pneumoniae* cells attached to SP4 growth medium-coated glass coverslips (Fig. 17), establishing the scan parameters for visualizing the mycoplasmas by AFM. Significantly, resolution is sufficient to identify the terminal organelle on individual cells. We have also successfully measured binding force of α-2,3- and α-2,6-sialyllactose-functionalized probes with the sialic acid-specific lectin WGA coated on glass coverslips (Table 4). Our results show that the functionalized AFM tip retains the capacity to bind to the WGA (Table 4).

In the future we will functionalize AFM tips with α-2,3-sialyllactose, α-2,6-sialyllactose, and lactose sulfate to measure the binding force between live *M. pneumoniae* cells and each receptor. This will also generate topographic heat maps of the cell surface that indicate where the strongest binding between receptor and adhesin occurs on the cell. We believe that α-2,3- and α-2,6-sialyllactose receptors will have different binding forces, indicated by the difference in attachment levels seen on functionalized surfaces. However, we hypothesize that they will exhibit similar results for the topographic heat maps, indicating use of the same adhesin complex. For the lactose

Table 4. Binding force of sialyllactose and wheat germ agglutinin. Binding force measurements between sialyllactose-coated atomic force microscope tips and surfaces coated with wheat germ agglutinin.

α-2,6-sialyllactose		**α-2,3-sialyllactose**	
Loading Rate (nN/s)	**Force (pN)**	**Loading Rate (nN/s)**	**Force (pN)**
20.1	39.7	2.08	25.8
54	40.73	4.16	33.3
102.7	46.71	6.25	41.6
201	54.88	12.50	48.5
500	57.65	14.28	54.8

sulfate, we speculate that binding force could be high compared to α-2,3-sialyllactose, indicating that non-motility seen on sulfatide is due to a high binding affinity between receptor and adhesin complex preventing the "catch" and "release" mechanism necessary for gliding. It is also possible that sulfatide may interact with a completely different adhesin complex than α-2,3- or α-2,6-sialyllactose. The P30 mutants have nonfunctional P1 despite it localizing properly to the terminal organelle, leading to a nonfunctional P1 adhesin complex (3). The high levels of attachment of the II-3 mutant to sulfatide indicates that the P1 adhesin complex does not play a role in receptor binding to sulfated receptors, making an alternate adhesin more likely. Interaction of the sulfated receptor across the whole cell surface, and not isolated to the terminal organelle, could indicate the use of an adhesin other than P1, that does not play a role in gliding motility.

Receptor specificity and pathogenesis in human airways

The studies presented here aimed to elucidate the interaction of *M. pneumoniae* and the host via the study of sialylated and sulfated receptor populations *in vitro*. Both sialylated and sulfated receptors play a role in interaction with the host for other mycoplasma species, as well as other human respiratory pathogens. Notably, the interaction of influenza and sialylated receptors in the airway has been studied extensively. It has been shown that α-2,6-sialylated glycans, a primary target of human influenza, and α-2,3-sialylated glycans, a primary target of avian influenza, can be found on normal human bronchial epithelial cells (212). However, binding of influenza virus to these sialylated receptors appears to be nuanced, with binding to α-2,3- and α-2,6 sialylated receptors, which may also be true for receptor recognition by *M. pneumoniae* (216, 217). Previous studies utilized lectin histochemistry to elucidate the presence,

relative abundance, and distribution of α-2,3- and α-2,6 sialylated receptors in the airway. The studies showed that α-2,6-sialylated glycans are more abundant in the upper respiratory tract (178), while α-2,3-sialylated glycan abundance is greater in the bronchial epithelium (218). Interestingly, a difference was seen in the abundance of α-2,6-sialylated glycans and α-2,3-sialylated glycans on ciliated verse non-ciliated cells, as well (219). When observing binding of α-2,6- and α-2,3-sialyl specific lectins on airway epithelial cells, α-2,6-sialyllated glycans were present on non-ciliated cells while α-2,3-siaylated glycans were present on most ciliated cells (219). Studies by Prince et. al. (10) showed that *M. pneumoniae* colonizes normal human bronchial epithelium (NHBE) cells beginning with attachment to the tips of the cilia, followed by rapid downward movement to the base of the cilia at the cell surface. However, *M. pneumoniae* exhibits slower lateral spread to neighboring non-ciliated cells. It is possible that the different nature of receptors found on the ciliated verse non-ciliated cells allows for rapid movement to the base of the cilia and slower spread from there, perhaps due to the higher density of α-2,6-sialyl linkages. The difference in gliding phenotype on α-2,3- and α-2,6 sialylated receptors indicates that receptors could act to promote gliding or act as a barrier. As glycan analysis reveals more information about the surface environment of the airway mucosa, it will be possible to define further how the receptor environment influences *M. pneumoniae* attachment and gliding behavior and ultimately impacting infection outcome.

REFERENCES

1. Waites KB, Atkinson PT. 2009. The role of Mycoplasma in upper respiratory infections. Current infectious disease reports 11.
2. Waites KB, Balish MF, Atkinson TP. 2008. New insights into the pathogenesis and detection of Mycoplasma pneumoniae infections. Future Microbiol 3:635-48.
3. Romero-Arroyo CE, Jordan J, Peacock SJ, Willby MJ, Farmer MA, Krause DC. 1999. Mycoplasma pneumoniae protein P30 is required for cytadherence and associated with proper cell development. J Bacteriol 181:1079-1087.
4. Krunkosky TM, Jordan JL, Kyung P, Krause DC, How-Yi C. 2007. Virulence Mechanisms of Bacterial Pathogens, Fourth Edition. highwire:135-147.
5. Jordan JL, Chang HY, Balish MF, Holt LS, Bose SR, Hasselbring BM, Waldo RH, 3rd, Krunkosky TM, Krause DC. 2007. Protein P200 is dispensable for Mycoplasma pneumoniae hemadsorption but not gliding motility or colonization of differentiated bronchial epithelium. Infect Immun 75:518-22.
6. Szczepanek SM, Majumder S, Sheppard ES, Liao X, Rood D, Tulman ER, Wyand S, Krause DC, Silbart LK, Geary SJ. 2012. Vaccination of BALB/c mice with an avirulent Mycoplasma pneumoniae P30 mutant results in disease exacerbation upon challenge with a virulent strain. Infect Immun 80:1007-1014.
7. Cloward JM, Krause DC. 2009. Mycoplasma pneumoniae J-domain protein required for terminal organelle function. Mol Microbiol 71.

8. Krause DC, Leith DK, Wilson RM, Baseman JB. 1982. Identification of Mycoplasma pneumoniae proteins associated with hemadsorption and virulence. Infect Immun 35:809-17.

9. Fraser CM, Gocayne JD, White O, Adams MD, Clayton RA, Fleischmann RD, Bult CJ, Kerlavage AR, Sutton G, Kelley JM, Fritchman RD, Weidman JF, Small KV, Sandusky M, Fuhrmann J, Nguyen D, Utterback TR, Saudek DM, Phillips CA, Merrick JM, Tomb JF, Dougherty BA, Bott KF, Hu PC, Lucier TS, Peterson SN, Smith HO, Hutchison CA, 3rd, Venter JC. 1995. The minimal gene complement of Mycoplasma genitalium. Science 270:397-403.

10. Prince OA, Krunkosky TM, Krause DC. 2014. In vitro spatial and temporal analysis of Mycoplasma pneumoniae colonization of human airway epithelium. Infect Immun 82:579-86.

11. Jaffe JD, Miyata M, Berg HC. 2004. Energetics of gliding motility in Mycoplasma mobile. J Bacteriol 186:4254-61.

12. Atkinson TP, Balish MF, Waites KB. 2008. Epidemiology, clinical manifestations, pathogenesis and laboratory detection of Mycoplasma pneumoniae infections. FEMS Microbiol Rev 32:956-73.

13. Nisar N, Guleria R, Kumar S, Chand Chawla T, Ranjan Biswas N. 2007. Mycoplasma pneumoniae and its role in asthma. Postgrad Med J 83:100-4.

14. Krivan HC, Olson LD, Barile MF, Ginsburg V, Roberts DD. 1989. Adhesion of Mycoplasma pneumoniae to sulfated glycolipids and inhibition by dextran sulfate. J Biol Chem 264:9283-8.

15. Roberts DD, Olson LD, Barile MF, Ginsburg V, Krivan HC. 1989. Sialic acid-dependent adhesion of Mycoplasma pneumoniae to purified glycoproteins. J Biol Chem 264:9289-93.

16. Sobeslavsky O, Prescott B, Chanock RM. 1968. Adsorption of Mycoplasma pneumoniae to neuraminic acid receptors of various cells and possible role in virulence. J Bacteriol 96:695-705.

17. Kasai T, Nakane D, Ishida H, Ando H, Kiso M, Miyata M. 2013. Role of binding in Mycoplasma mobile and Mycoplasma pneumoniae gliding analyzed through inhibition by synthesized sialylated compounds. J Bacteriol 195:429-35.

18. Razin S. 2006. The Genus Mycoplasma and Related Genera (Class Mollicutes). *In* Dworkin M, Falkow S, Rosenberg E, Schleifer K, Stackebrandt E (ed), The Prokaryotes. Springer, New York, NY.

19. Razin S. 1978. The mycoplasmas. The mycoplasmas 42.

20. Maniloff J. 2002. Phylogeny and evolution. *In* Razin S, Herrmann R (ed), Molecular Biology and Pathogenicity of Mycoplasmas. Springer, Boston, MA.

21. Razin S, Yogev D, Naot Y. 1998. Molecular Biology and Pathogenicity of Mycoplasmas. 62.

22. Pollack DJ. 2002. Central carbohydrate pathways: Metabolic flexibility and the extra role of some “housekeeping” enzymes. Springer.

23. Razin S, Hayflick L. 2010. Highlights of Mycoplasma Research - An Historical Perspective. Biologicals 38:183-190.

24. Schuster S, Pfeiffer T, Moldenhauer F, Koch I, Dandekar T. 2002. Exploring the pathway structure of metabolism: decomposition into subnetworks and application to Mycoplasma pneumoniae. Bioinformatics 18:351-61.

25. Himmelreich R, Hilbert H, Plagens H, Pirkl E, Li BC, Herrmann R. 1996. Complete sequence analysis of the genome of the bacterium Mycoplasma pneumoniae. Nucleic Acids Res 24:4420-49.

26. Razin S, Tully JG. 1970. Cholesterol requirement of mycoplasmas. J Bacteriol 102:306-10.

27. Razin S. 1967. The cell membrane of mycoplasma. Ann N Y Acad Sci 143:115-29.

28. Razin S. 1969. Structure and function in mycoplasma. Annu Rev Microbiol 23:317-56.

29. Eaton MD, Meiklejohn G, van Herick W. 1944. Studies on the Etiology of Primary Atypical Pneumonia : A Filterable Agent Transmissible to Cotton Rats, Hamsters, and Chick Embryos. J Exp Med 79:649-68.

30. Saraya T. 2016. The History of Mycoplasma pneumoniae Pneumonia. Front Microbiology 7:364.

31. Eaton MD, Meikeljohn G, Vanherick W, Talbot JC. 1942. An Infectious Agent from Cases of Atypical Pneumonia Apparently Transmissible to Cotton Rats. Science 96:518-9.

32. Eaton MD, Meiklejohn G, van Herick W, Corey M. 1945. Studies on the Etiology of Primary Atypical Pneumonia : Ii. Properties of the Virus Isolated and Propagated in Chick Embryos. J Exp Med 82:317-28.

33. Eaton MD. 1950. Action of aureomycin and chloromycetin on the virus of primary atypical pneumonia. Proc Soc Exp Biol Med 73:24-9.

34. Clyde WA, Jr. 1963. Studies on growth of Eaton's agent in tissue culture. Proc Soc Exp Biol Med 112:905-9.

35. Liu C. 1957. Studies on primary atypical pneumonia. I. Localization, isolation, and cultivation of a virus in chick embryos. J Exp Med 106:455-66.

36. Liu C, Eaton MD, Heyl JT. 1959. Studies on primary atypical pneumonia. II. Observations concerning the development and immunological characteristics of antibody in patients. J Exp Med 109:545-56.

37. Chanock RM, Hayflick L, Barile MF. 1962. Growth on artificial medium of an agent associated with atypical pneumonia and its identification as a PPLO. Proc Natl Acad Sci U S A 48:41-9.

38. Eaton MD, Liu C. 1957. Studies on sensitivity to streptomycin of the atypical pneumonia agent. J Bacteriol 74:784-7.

39. Kingston JR, Chanock RM, Mufson MA, Hellman LP, James WD, Fox HH, Manko MA, Boyers J. 1961. Eaton agent pneumonia. JAMA 176:118-23.

40. Marmion BP, Goodburn GM. 1961. Effect of an organic gold salt on Eaton's primary atypical pneumonia agent and other observations. Nature 189:247-8.

41. Goodburn GM, Marmion BP. 1962. A study of the properties of Eaton's primary atypical pneumonia organism. J Gen Microbiol 29:271-90.

42. Chanock RM, Fox HH, James WD, Bloom HH, Mufson MA. 1960. Growth of laboratory and naturally occurring strains of Eaton agent in monkey kidney tissue culture. Proc Soc Exp Biol Med 105:371-5.

43. Clyde WA, Jr., Denny FW, Dingle JH. 1961. Fluorescent-stainable antibodies to the Eaton agent in human primary atypical pneumonia transmission studies. J Clin Invest 40:1638-47.

44. Chanock RM. 1963. Mycoplasma pneumoniae: proposed nomenclature for atypical pneumonia organism (Eaton agent). Science 140:662.

45. Waites KB, Talkington DF. 2004. Mycoplasma pneumoniae and Its Role as a Human Pathogen. Clin Microbiol Rev 17:697-728.

46. Waites KB, Xiao L, Liu Y, Balish MF, Atkinson TP. 2017. Mycoplasma pneumoniae from the Respiratory Tract and Beyond. Clin Microbiol Rev 30:747-809.

47. Lind K, Benzon MW, Jensen JS, Clyde WA, Jr. 1997. A seroepidemiological study of Mycoplasma pneumoniae infections in Denmark over the 50-year period 1946-1995. Eur J Epidemiol 13:581-6.

48. Foy HM, Grayston JT, Kenny GE, Alexander ER, McMahan R. 1966. Epidemiology of Mycoplasma pneumoniae infection in families. JAMA 197:859-66.

49. Foy HM. 1993. Infections caused by Mycoplasma pneumoniae and possible carrier state in different populations of patients. Clin Infect Dis 17 Suppl 1:S37-46.

50. Alexander ER, Foy HM, Kenny GE, Kronmal RA, McMahan R, Clarke ER, MacColl WA, Grayston JT. 1966. Pneumonia due to Mycoplasma pneumoniae. Its incidence in the membership of a co-operative medical group. N Engl J Med 275:131-6.

51. Wubbel L, Muniz L, Ahmed A, Trujillo M, Carubelli C, McCoig C, Abramo T, Leinonen M, McCracken GH, Jr. 1999. Etiology and treatment of community-acquired pneumonia in ambulatory children. Pediatr Infect Dis J 18:98-104.

52. Ieven M, Ursi D, Van Bever H, Quint W, Niesters HG, Goossens H. 1996. Detection of Mycoplasma pneumoniae by two polymerase chain reactions and role of M. pneumoniae in acute respiratory tract infections in pediatric patients. J Infect Dis 173:1445-52.

53. Harris JA, Kolokathis A, Campbell M, Cassell GH, Hammerschlag MR. 1998. Safety and efficacy of azithromycin in the treatment of community-acquired pneumonia in children. Pediatr Infect Dis J 17:865-71.

54. Block S, Hedrick J, Hammerschlag MR, Cassell GH, Craft JC. 1995. Mycoplasma pneumoniae and Chlamydia pneumoniae in pediatric community-acquired pneumonia: comparative efficacy and safety of clarithromycin vs. erythromycin ethylsuccinate. Pediatr Infect Dis J 14:471-7.

55. Hammerschlag MR. 1995. Atypical pneumonias in children. Adv Pediatr Infect Dis 10:1-39.

56. Marrie TJ. 1999. Pneumococcal pneumonia: epidemiology and clinical features. Semin Respir Infect 14:227-36.

57. Esposito S, Bosis S, Cavagna R, Faelli N, Begliatti E, Marchisio P, Blasi F, Bianchi C, Principi N. 2002. Characteristics of Streptococcus pneumoniae and atypical bacterial infections in children 2-5 years of age with community-acquired pneumonia. Clin Infect Dis 35:1345-52.

58. Ferwerda A, Moll HA, de Groot R. 2001. Respiratory tract infections by Mycoplasma pneumoniae in children: a review of diagnostic and therapeutic measures. Eur J Pediatr 160:483-91.

59. Luby JP. 1991. Pneumonia caused by Mycoplasma pneumoniae infection. Clin Chest Med 12:237-44.

60. Stevens D, Swift PG, Johnston PG, Kearney PJ, Corner BD, Burman D. 1978. Mycoplasma pneumoniae infections in children. Arch Dis Child 53:38-42.

61. Smith CB, Golden CA, Kanner RE, Renzetti AD, Jr. 1980. Association of viral and Mycoplasma pneumoniae infections with acute respiratory illness in patients with chronic obstructive pulmonary diseases. Am Rev Respir Dis 121:225-32.

62. Smith CB, Kanner RE, Golden CA, Klauber MR, Renzetti AD, Jr. 1980. Effect of viral infections on pulmonary function in patients with chronic obstructive pulmonary diseases. J Infect Dis 141:271-80.

63. Gump DW, Phillips CA, Forsyth BR, McIntosh K, Lamborn KR, Stouch WH. 1976. Role of infection in chronic bronchitis. Am Rev Respir Dis 113:465-74.

64. Buscho RO, Saxtan D, Shultz PS, Finch E, Mufson MA. 1978. Infections with viruses and Mycoplasma pneumoniae during exacerbations of chronic bronchitis. J Infect Dis 137:377-83.

65. Esposito S, Cavagna R, Bosis S, Droghetti R, Faelli N, Principi N. 2002. Emerging role of Mycoplasma pneumoniae in children with acute pharyngitis. Eur J Clin Microbiol Infect Dis 21:607-10.

66. Lee RE, Kaza S, Plano GV, Casiano RR. 2005. The role of atypical bacteria in chronic rhinosinusitis. Otolaryngol Head Neck Surg 133:407-10.

67. Savolainen S, Jousimies-Somer H, Kleemola M, Ylikoski J. 1989. Serological evidence of viral or Mycoplasma pneumoniae infection in acute maxillary sinusitis. Eur J Clin Microbiol Infect Dis 8:131-5.

68. Gurr PA, Chakraverty A, Callanan V, Gurr SJ. 1996. The detection of Mycoplasma pneumoniae in nasal polyps. Clin Otolaryngol Allied Sci 21:269-73.

69. Bar Meir E, Amital H, Levy Y, Kneller A, Bar-Dayan Y, Shoenfeld Y. 2000. Mycoplasma-pneumoniae-induced thrombotic thrombocytopenic purpura. Acta haematologica 103:112-115.

70. Kasahara I, Otsubo Y, Yanase T, Oshima H, Ichimaru H, Nakamura M. 1985. Isolation and characterization of Mycoplasma pneumoniae from cerebrospinal fluid of a patient with pneumonia and meningoencephalitis. J Infect Dis 152:823-5.

71. Koletsky RJ, Weinstein AJ. 1980. Fulminant Mycoplasma pneumoniae infection. Report of a fatal case, and a review of the literature. Am Rev Respir Dis 122:491-6.

72. Said MH, Layani MP, Colon S, Faraj G, Glastre C, Cochat P. 1999. Mycoplasma pneumoniae-associated nephritis in children. Pediatr Nephrol 13:39-44.

73. Wood PR, Kampschmidt JC, Dube PH, Cagle MP, Chaparro P, Ketchum NS, Kannan TR, Singh H, Peters JI, Baseman JB, Brooks EG. 2017. Mycoplasma pneumoniae and health outcomes in children with asthma. Ann Allergy Asthma Immunol 119:146-152 e2.

74. Wood PR, Hill VL, Burks ML, Peters JI, Singh H, Kannan TR, Vale S, Cagle MP, Principe MF, Baseman JB, Brooks EG. 2013. Mycoplasma pneumoniae in

children with acute and refractory asthma. Ann Allergy Asthma Immunol 110:328-334 e1.

75. Cassell GH. 1998. Infectious causes of chronic inflammatory diseases and cancer. Emerg Infect Dis 4:475-87.

76. Lieberman D, Lieberman D, Printz S, Ben-Yaakov M, Lazarovich Z, Ohana B, Friedman MG, Dvoskin B, Leinonen M, Boldur I. 2003. Atypical pathogen infection in adults with acute exacerbation of bronchial asthma. Am J Respir Crit Care Med 167:406-10.

77. Seggev JS, Lis I, Siman-Tov R, Gutman R, Abu-Samara H, Schey G, Naot Y. 1986. Mycoplasma pneumoniae is a frequent cause of exacerbation of bronchial asthma in adults. Ann Allergy 57:263-5.

78. Kraft M, Cassell GH, Henson JE, Watson H, Williamson J, Marmion BP, Gaydos CA, Martin RJ. 1998. Detection of Mycoplasma pneumoniae in the airways of adults with chronic asthma. Am J Respir Crit Care Med 158:998-1001.

79. Shimizu T, Mochizuki H, Kato M, Shigeta M, Morikawa A, Hori T. 1991. [Immunoglobulin levels, number of eosinophils in the peripheral blood and bronchial hypersensitivity in children with Mycoplasma pneumoniae pneumonia]. Arerugi 40:21-7.

80. Esposito S, Droghetti R, Bosis S, Claut L, Marchisio P, Principi N. 2002. Cytokine secretion in children with acute Mycoplasma pneumoniae infection and wheeze. Pediatr Pulmonol 34:122-7.

81. Hardy RD, Jafri HS, Olsen K, Wordemann M, Hatfield J, Rogers BB, Patel P, Duffy L, Cassell G, McCracken GH, Ramilo O. 2001. Elevated cytokine and

chemokine levels and prolonged pulmonary airflow resistance in a murine Mycoplasma pneumoniae pneumonia model: a microbiologic, histologic, immunologic, and respiratory plethysmographic profile. Infect Immun 69:3869-76.

82. Biberfeld G, Biberfeld P. 1970. Ultrastructural features of Mycoplasma pneumoniae. J Bacteriol 102:855-61.

83. Bredt W. 1968. Growth morphology of Mycoplasma pneumoniae strain FH on glass surface. Proc Soc Exp Biol Med 128:338-40.

84. Kim J, Copley SD. 2012. Inhibitory cross-talk upon introduction of a new metabolic pathway into an existing metabolic network. 109.

85. Krause DC, Balish MF. 2004. MicroReview Cellular engineering in a minimal microbe: structure and assembly of the terminal organelle of Mycoplasma pneumoniae. Mol Microbiol 51:917-924.

86. Balish MF. 2014. Mycoplasma pneumoniae, an underutilized model for bacterial cell biology. J Bacteriol 196:3675-3682.

87. Nakane D, Kenri T, Matsuo L, Miyata M. 2015. Systematic Structural Analyses of Attachment Organelle in Mycoplasma pneumoniae. PLoS Pathog 11:e1005299.

88. Hegermann J, Herrmann R, Mayer F. 2002. Cytoskeletal elements in the bacterium Mycoplasma pneumoniae. Naturwissenschaften 89:453-8.

89. Meng KE, Pfister RM. 1980. Intracellular structures of Mycoplasma pneumoniae revealed after membrane removal. J Bacteriol 144:390-9.

90. Regula JT, Boguth G, Gorg A, Hegermann J, Mayer F, Frank R, Herrmann R. 2001. Defining the mycoplasma 'cytoskeleton': the protein composition of the

Triton X-100 insoluble fraction of the bacterium Mycoplasma pneumoniae determined by 2-D gel electrophoresis and mass spectrometry. Microbiology 147:1045-57.

91. Seybert A, Herrmann R, Frangakis AS. 2006. Structural analysis of Mycoplasma pneumoniae by cryo-electron tomography. J Struct Biol 156:342-54.

92. Henderson GP, Jensen GJ. 2006. Three-dimensional structure of Mycoplasma pneumoniae's attachment organelle and a model for its role in gliding motility. Mol Microbiol 60:376-85.

93. Seto S, Miyata M. 2003. Attachment organelle formation represented by localization of cytadherence proteins and formation of the electron-dense core in wild-type and mutant strains of Mycoplasma pneumoniae. J Bacteriol 185:1082-91.

94. Bose SR, Balish MF, Krause DC. 2009. Mycoplasma pneumoniae cytoskeletal protein HMW2 and the architecture of the terminal organelle. J Bacteriol 191:6741-8.

95. Kawamoto A, Matsuo L, Kato T, Yamamoto H, Namba K, Miyata M. 2016. Periodicity in Attachment Organelle Revealed by Electron Cryotomography Suggests Conformational Changes in Gliding Mechanism of Mycoplasma pneumoniae. mBio 7:16.

96. Willby MJ, Krause DC. 2002. Characterization of a Mycoplasma pneumoniae hmw3 mutant: implications for attachment organelle assembly. J Bacteriol 184:3061-8.

97. Balish MF, Santurri RT, Ricci AM, Lee KK, Krause DC. 2003. Localization of Mycoplasma pneumoniae cytadherence-associated protein HMW2 by fusion with green fluorescent protein: implications for attachment organelle structure. Mol Microbiol 47:49-60.

98. Krause DC, Shi J, Chen S, Jensen A, Sheppard ES, Jensen GJ. 2018. Electron cryotomography correlates *Mycoplasma pneumoniae* terminal organelle ultrastructural features and fucntion. Mol Microbiol.

99. Layh-Schmitt G, Herrmann R. 1992. Localization and biochemical characterization of the ORF6 gene product of the Mycoplasma pneumoniae P1 operon. Infect Immun 60:2906-13.

100. Willby MJ, Balish MF, Ross SM, Lee KK, Jordan JL, Krause DC. 2004. HMW1 is required for stability and localization of HMW2 to the attachment organelle of Mycoplasma pneumoniae. J Bacteriol 186:8221-8.

101. Jordan JL, Berry KM, Balish MF, Krause DC. 2001. Stability and subcellular localization of cytadherence-associated protein P65 in Mycoplasma pneumoniae. J Bacteriol 183:7387-91.

102. Popham PL, Hahn TW, Krebes KA, Krause DC. 1997. Loss of HMW1 and HMW3 in noncytadhering mutants of Mycoplasma pneumoniae occurs post-translationally. Proc Natl Acad Sci U S A 94:13979-13984.

103. Stevens MK, Krause DC. 1992. Mycoplasma pneumoniae cytadherence phase-variable protein HMW3 is a component of the attachment organelle. J Bacteriol 174:4265-74.

104. Proft T, Hilbert H, Layh-Schmitt G, Herrmann R. 1995. The proline-rich P65 protein of Mycoplasma pneumoniae is a component of the Triton X-100-insoluble fraction and exhibits size polymorphism in the strains M129 and FH. J Bacteriol 177:3370-8.

105. Kenri T, Seto S, Horino A, Sasaki Y, Sasaki T, Miyata M. 2004. Use of fluorescent-protein tagging to determine the subcellular localization of mycoplasma pneumoniae proteins encoded by the cytadherence regulatory locus. J Bacteriol 186:6944-55.

106. Seto S, Layh-Schmitt G, Kenri T, Miyata M. 2001. Visualization of the Attachment Organelle and Cytadherence Proteins of Mycoplasma pneumoniae by Immunofluorescence Microscopy. Journal of Bacteriology 183:1621-1630.

107. Jordan JL, Berry KM, Balish MF, Krause DC. 2001. Stability and subcellular localization of cytadherence-associated protein P65 in Mycoplasma pneumoniae. Journal of bacteriology 183:7387-7391.

108. Proft T, Herrmann R. 1994. Identification and characterization of hitherto unknown Mycoplasma pneumoniae proteins. Mol Microbiol 13:337-48.

109. Hasselbring BM, Sheppard ES, Krause DC. 2012. P65 truncation impacts P30 dynamics during Mycoplasma pneumoniae gliding. J Bacteriol 194.

110. Hasselbring BM, Krause DC. 2007. Proteins P24 and P41 function in the regulation of terminal-organelle development and gliding motility in Mycoplasma pneumoniae. J Bacteriol 189.

111. Hasselbring BM, Krause DC. 2007. Cytoskeletal protein P41 is required to anchor the terminal organelle of the wall-less prokaryote Mycoplasma pneumoniae. Proc Natl Acad Sci U S A 63:44-53.

112. Hasselbring BM, Krause DC. 2007. Cytoskeletal protein P41 is required to anchor the terminal organelle of the wall-less prokaryote Mycoplasma pneumoniae. Mol Microbiol 63:44-53.

113. Baseman JB, Cole RM, Krause DC, Leith DK. 1982. Molecular basis for cytadsorption of Mycoplasma pneumoniae. J Bacteriol 151:1514-22.

114. Feldner J, Gobel U, Bredt W. 1982. Mycoplasma pneumoniae adhesin localized to tip structure by monoclonal antibody. Nature 298:765-7.

115. Hu PC, Cole RM, Huang YS, Graham JA, Gardner DE, Collier AM, Clyde WA, Jr. 1982. Mycoplasma pneumoniae infection: role of a surface protein in the attachment organelle. Science 216:313-5.

116. Razin S, Jacobs E. 1992. Mycoplasma adhesion. J Gen Microbiol 138:407-22.

117. Franzoso G, Hu PC, Meloni GA, Barile MF. 1993. The immunodominant 90-kilodalton protein is localized on the terminal tip structure of Mycoplasma pneumoniae. Infect Immun 61:1523-30.

118. Sperker B, Hu P, Herrmann R. 1991. Identification of gene products of the P1 operon of Mycoplasma pneumoniae. Mol Microbiol 5:299-306.

119. Waldo RH, 3rd, Jordan JL, Krause DC. 2005. Identification and complementation of a mutation associated with loss of Mycoplasma pneumoniae virulence-specific proteins B and C. J Bacteriol 187:747-51.

120. Hasselbring BM, Jordan JL, Krause RW, Krause DC. 2006. Terminal organelle development in the cell wall-less bacterium Mycoplasma pneumoniae. Proc Natl Acad Sci U S A 103:16478-16483.

121. Waldo RH, 3rd, Krause DC. 2006. Synthesis, stability, and function of cytadhesin P1 and accessory protein B/C complex of Mycoplasma pneumoniae. J Bacteriol 188:569-75.

122. Layh-Schmitt G, Podtelejnikov A, Mann M. 2000. Proteins complexed to the P1 adhesin of Mycoplasma pneumoniae. Microbiology 146 (Pt 3):741-7.

123. Seto S, Kenri T, Tomiyama T, Miyata M. 2005. Involvement of P1 adhesin in gliding motility of Mycoplasma pneumoniae as revealed by the inhibitory effects of antibody under optimized gliding conditions. J Bacteriol 187:1875-7.

124. Cloward JM, Krause DC. 2011. Loss of co-chaperone TopJ impacts adhesin P1 presentation and terminal organelle maturation in Mycoplasma pneumoniae. Mol Microbiol 81:528-39.

125. Baseman JB, Morrison-Plummer J, Drouillard D, Puleo-Scheppke B, Tryon VV, Holt SC. 1987. Identification of a 32-kilodalton protein of Mycoplasma pneumoniae associated with hemadsorption. Isr J Med Sci 23:474-9.

126. Hasselbring BM, Jordan JL, Krause DC. 2005. Mutant analysis reveals a specific requirement for protein P30 in Mycoplasma pneumoniae gliding motility. J Bacteriol 187:6281-9.

127. Chang H-Y, a Prince O, Sheppard ES, Krause DC. 2011. Processing is required for a fully functional protein P30 in Mycoplasma pneumoniae gliding and cytadherence. J Bacteriol 193.

128. Krunkosky TM, Jordan JL, Chambers E, Krause DC. 2007. Mycoplasma pneumoniae host-pathogen studies in an air-liquid culture of differentiated human airway epithelial cells. Microb Pathog 42:98-103.

129. Miyata M, Hamaguchi T. 2016. Integrated Information and Prospects for Gliding Mechanism of the Pathogenic Bacterium Mycoplasma pneumoniae. Front Microbiology 7:960.

130. Dallo SF, Lazzell AL, Chavoya A, Reddy SP, Baseman JB. 1996. Biofunctional domains of the Mycoplasma pneumoniae P30 adhesin. Infect Immun 64:2595-601.

131. Cloward JM, Krause DC. 2010. Functional domain analysis of the Mycoplasma pneumoniae co-chaperone TopJ. Mol Microbiol 77:158-169.

132. Miyata M. 2010. Unique centipede mechanism of Mycoplasma gliding. Annu Rev Microbiol 64:519-37.

133. Davis JJ, Xia F, Overbeek RA, Olsen GJ. 2013. Genomes of the class Erysipelotrichia clarify the firmicute origin of the class Mollicutes. Int J Syst Evol Microbiol 63:2727-41.

134. Jarrell KF, McBride MJ. 2008. The surprisingly diverse ways that prokaryotes move. Nat Rev Microbiol 6:466.

135. Nakane D, Miyata M. 2009. Cytoskeletal asymmetrical dumbbell structure of a gliding mycoplasma, Mycoplasma gallisepticum, revealed by negative-staining electron microscopy. J Bacteriol 191:3256-3264.

136. Uenoyama A, Miyata M. 2005. Gliding ghosts of Mycoplasma mobile. Proc Natl Acad Sci U S A 102:12754-8.

137. Kinosita Y, Nakane D, Sugawa M, Masaike T, Mizutani K, Miyata M, Nishizaka T. 2014. Unitary step of gliding machinery in Mycoplasma mobile. Proc Natl Acad Sci U S A 111:8601-6.

138. Hasselbring BM, a Page C, Sheppard ES, Krause DC. 2006. Transposon mutagenesis identifies genes associated with Mycoplasma pneumoniae gliding motilityJ Bacteriol 188.

139. Page CA, Krause DC. 2013. Protein kinase/phosphatase function correlates with gliding motility in Mycoplasma pneumoniae. J Bacteriol 195:1750-7.

140. Schmidl SR, Gronau K, Hames C, Busse J, Becher D, Hecker M, Stulke J. 2010. The stability of cytadherence proteins in Mycoplasma pneumoniae requires activity of the protein kinase PrkC. Infect Immun 78:184-92.

141. Baseman JB, Lange M, Criscimagna NL, Giron JA, Thomas CA. 1995. Interplay between mycoplasmas and host target cells. Microb Pathog 19:105-16.

142. Dallo SF, Baseman JB. 2000. Intracellular DNA replication and long-term survival of pathogenic mycoplasmas. Microb Pathog 29:301-9.

143. Collier AM, Clyde WA. 1971. Relationships Between Mycoplasma pneumoniae and Human Respiratory Epithelium. Infect Immun 3:694-701.

144. Powell DA, Hu PC, Wilson M, Collier AM, Baseman JB. 1976. Attachment of Mycoplasma pneumoniae to respiratory epithelium. Infect Immun 13:959-66.

145. Wilson MH, Collier AM. 1976. Ultrastructural study of Mycoplasma pneumoniae in organ culture. J Bacteriol 125:332-9.

146. Prince OA, Krunkosky TM, Sheppard ES, Krause DC. 2018. Modelling persistent Mycoplasma pneumoniae infection of human airway epithelium. Cell Microbiol 20.

147. Somerson NL, Walls BE, Chanock RM. 1965. Hemolysin of Mycoplasma pneumoniae: tentative identification as a peroxide. Science 150:226-8.

148. Brennan PC, Feinstein RN. 1969. Relationship of hydrogen peroxide production by Mycoplasma pulmonis to virulence for catalase-deficient mice. J Bacteriol 98:1036-40.

149. Simmons WL, Dybvig K. 2015. Catalase Enhances Growth and Biofilm Production of Mycoplasma pneumoniae. Curr Microbiol 71:190-4.

150. McAuliffe L, Ellis RJ, Miles K, Ayling RD, Nicholas RA. 2006. Biofilm formation by mycoplasma species and its role in environmental persistence and survival. Microbiology 152:913-22.

151. Kornspan JD, Tarshis M, Rottem S. 2011. Adhesion and biofilm formation of Mycoplasma pneumoniae on an abiotic surface. Arch Microbiol 193:833-6.

152. García-Castillo M, Morosini M-I, Gálvez M, Baquero F, Campo R, Meseguer M-A. 2008. Differences in biofilm development and antibiotic susceptibility among clinical Ureaplasma urealyticum and Ureaplasma parvum isolates. J Antimicrob Chemother 62:1027-1030.

153. Simmons WL, Bolland JR, Daubenspeck JM, Dybvig K. 2007. A stochastic mechanism for biofilm formation by Mycoplasma pulmonis. J Bacteriol 189:1905-13.

154. Simmons WL, Dybvig K. 2007. Biofilms protect Mycoplasma pulmonis cells from lytic effects of complement and gramicidin. Infect Immun 75:3696-9.

155. Simmons WL, Dybvig K. 2009. Mycoplasma biofilms ex vivo and in vivo. FEMS Microbiol Lett 295:77-81.

156. Simmons WL, Daubenspeck JM, Osborne JD, Balish MF, Waites KB, Dybvig K. 2013. Type 1 and type 2 strains of Mycoplasma pneumoniae form different biofilms. Microbiology 159:737-47.

157. Kannan TR, Baseman JB. 2006. ADP-ribosylating and vacuolating cytotoxin of Mycoplasma pneumoniae represents unique virulence determinant among bacterial pathogens. Proc Natl Acad Sci U S A 103:6724-6729.

158. Krishnan M, Kannan TR, Baseman JB. 2013. Mycoplasma pneumoniae CARDS toxin is internalized via clathrin-mediated endocytosis. PloS one 8.

159. Su CJ, Chavoya A, Dallo SF, Baseman JB. 1990. Sequence divergency of the cytadhesin gene of Mycoplasma pneumoniae. Infect Immun 58:2669-74.

160. Su CJ, Dallo SF, Chavoya A, Baseman JB. 1993. Possible origin of sequence divergence in the P1 cytadhesin gene of Mycoplasma pneumoniae. Infect Immun 61:816-22.

161. Shimizu T. 2016. Inflammation-inducing factors of Mycoplasma pneumoniae. Front Microbiol 7.

162. Chan ED, Welsh CH. 1995. Fulminant Mycoplasma pneumoniae pneumonia. West J Med 162:133-42.

163. Opitz O, Pietsch K, Ehlers S, Jacobs E. 1997. Cytokine gene expression in immune mice reinfected with Mycoplasma pneumoniae: The role of T cells subsets in aggravating the inflammatory response. Immunobiology 196:575-587.

164. Fernald GW. 1972. In vitro response of human lymphocytes to Mycoplasma pneumoniae. Infect Immun 5:552-8.

165. Martin RR, Warr G, Couch R, Knight V. 1973. Chemotaxis of human leukocytes: responsiveness to Mycoplasma pneumoniae. J lab Clin Med 81:520-9.

166. Nakayama T, Urano T, Osano M, Maehara N, Makino S. 1986. Alpha interferon in the sera of patients infected with Mycoplasma pneumoniae. J Infect Dis 154:904-6.

167. Monto AS, Bryan ER, Rhodes LM. 1974. The Tecumseh study of respiratory illness. VII. Further observations on the occurrence of respiratory syncytial virus and Mycoplasma pneumoniae infections. Am J Epidemiol 100:458-68.

168. Sillis M. 1990. The limitations of IgM assays in the serological diagnosis of Mycoplasma pneumoniae infections. J Med Microbiol 33:253-8.

169. Granstrom M, Holme T, Sjogren AM, Ortqvist A, Kalin M. 1994. The role of IgA determination by ELISA in the early serodiagnosis of Mycoplasma pneumoniae infection, in relation to IgG and mu-capture IgM methods. J Med Microbiol 40:288-92.

170. Watkins-Riedel T, Stanek G, Daxboeck F. 2001. Comparison of SeroMP IgA with four other commercial assays for serodiagnosis of Mycoplasma pneumoniae pneumonia. Diagn Microbiol Infect Dis 40:21-5.

171. Hardy RD, Jafri HS, Olsen K, Hatfield J, Iglehart J, Rogers BB, Patel P, Cassell G, McCracken GH, Ramilo O. 2002. Mycoplasma pneumoniae induces chronic respiratory infection, airway hyperreactivity, and pulmonary inflammation: a murine model of infection-associated chronic reactive airway disease. Infect Immun 70:649-54.

172. Meakins JF. 1943. Primary Atypical Pneumonia of Unknown Etiology. Can Med Assoc J 48:333-7.

173. Banai M, Razin S, Bredt W, Kahane I. 1980. Isolation of binding sites to glycophorin from Mycoplasma pneumoniae membranes. Infect Immun 30:628-34.

174. Feldner J, Bredt W, Razin S. 1979. Adherence of Mycoplasma pneumoniae to glass surfaces. Infect Immun 26:70-5.

175. Gabridge MG, Barden-Stahl YD, Polisky RB, Engelhardt JA. 1977. Differences in the attachment of Mycoplasma pneumoniae cells and membranes to tracheal epithelium. Infect Immun 16:766-72.

176. Gabridge MG, Gunderson H, Schaeffer SL, Barden-Stahl YD. 1978. Ciliated respiratory epithelial monolayers: new model for Mycoplasma pneumoniae infection. Infect Immun 21:333-6.

177. Gabridge MG, Taylor-Robinson D. 1979. Interaction of Mycoplasma pneumoniae with human lung fibroblasts: role of receptor sites. Infect Immun 25:455-459.

178. Shinya K, Ebina M, Yamada S, Ono M, Kasai N, Kawaoka Y. 2006. Avian flu: influenza virus receptors in the human airway. Nature 440:435-6.

179. Nagai R, Miyata M. 2006. Gliding motility of Mycoplasma mobile can occur by repeated binding to N-acetylneuraminyllactose (sialyllactose) fixed on solid surfaces. J Bacteriol 188:6469-75.

180. Loveless RW, Feizi T. 1989. Sialo-oligosaccharide receptors for Mycoplasma pneumoniae and related oligosaccharides of poly-N-acetyllactosamine series are polarized at the cilia and apical-microvillar domains of the ciliated cells in human bronchial epithelium. Infect Immun 57:1285-9.

181. Loveless RW, Griffiths S, Fryer PR, Blauth C, Feizi T. 1992. Immunoelectron Microscopic Studies Reveal Differences in Distribution of Sialo-Oligosaccharide Receptors for Mycoplasma pneumoniae on the Epithelium of Human and Hamster Bronchi. Infect Immun 60:4015-4023.

182. Feldner J, Bredt W, Razin S. 1981. Role of energy metabolism in Mycoplasma pneumoniae attachment to glass surfaces. Infect Immun 31:107-113.

183. Weinbach EC, Garbus J. 1968. Structural changes in mitochondria induced by uncoupling reagents. The response to proteolytic enzymes. Biochem J 106:711-7.

184. Harold FM. 1977. Ion currents and physiological functions in microorganisms. Annu Rev Microbiol 31:181-203.

185. Banai M, Kahane I, Razin S, Bredt W. 1978. Adherence of Mycoplasma gallisepticum to human erythrocytes. Infect Immun 21:365-72.

186. Olson LD, Gilbert AA. 1993. Characteristics of Mycoplasma hominis adhesion. J Bacteriol 175:3224-7.

187. Zhang Q, Young TF, Ross RF. 1994. Glycolipid receptors for attachment of Mycoplasma hyopneumoniae to porcine respiratory ciliated cells. Infect Immun 62:4367-73.

188. Zhang Q, Young TF, Ross RF. 1994. Microtiter plate adherence assay and receptor analogs for Mycoplasma hyopneumoniae. Infect Immun 62:1616-22.

189. Brennan MJ, Hannah JH, Leininger E. 1991. Adhesion of Bordetella pertussis to sulfatides and to the GalNAc beta 4Gal sequence found in glycosphingolipids. J Biol Chem 266:18827-31.

190. Barthelson R, Mobasseri A, Zopf D, Simon P. 1998. Adherence of Streptococcus pneumoniae to respiratory epithelial cells is inhibited by sialylated oligosaccharides. Infect Immun 66:1439-44.

191. Garcia-Sastre A. 2010. Influenza virus receptor specificity: disease and transmission. Am J Pathol 176:1584-5.

192. Nilsson CL. 2003. Lectins: proteins that interpret the sugar code. Anal Chem 75:348A-353A.

193. Sharon N, Lis H. 2004. History of lectins: from hemagglutinins to biological recognition molecules. Glycobiology 14.

194. Lis H, reviews S-N. 1998. Lectins: carbohydrate-specific proteins that mediate cellular recognition. Chem Rev.

195. Weis WI, Drickamer K. 1996. Structural basis of lectin-carbohydrate recognition. Annu Rev Biochem 65:441-73.

196. Varki A. 1993. Biological roles of oligosaccharides: all of the theories are correct. Glycobiology 3:97-130.

197. Kiessling LL, Pohl NL. 1996. Strength in numbers: non-natural polyvalent carbohydrate derivatives. Chemistry & Biology 3:71-77.

198. Kiessling LL, in Biology L-AC. 2003. Multivalency in biological systems. Chemical Probes in Biology.

199. Kiessling LL, Pohl NL. 1996. Strength in numbers: non-natural polyvalent carbohydrate derivatives. Chem Biol 3:71-77.

200. Deng SJ, MacKenzie CR, Hirama T, Brousseau R, Lowary TL, Young NM, Bundle DR, Narang SA. 1995. Basis for selection of improved carbohydrate-binding single-chain antibodies from synthetic gene libraries. Proc Natl Acad Sci U S A 92:4992-6.

201. Eaton BE, Gold L, Zichi DA. 1995. Let's get specific: the relationship between specificity and affinity. Chem Biol 2:633-638.

202. Rini JM, Hardman KD, Einspahr H, Suddath FL, Carver JP. 1993. X-ray crystal structure of a pea lectin-trimannoside complex at 2.6 A resolution. J Biol Chem 268:10126-32.

203. Lipman RP, Clyde WA, Denny FW. 1969. Characteristics of virulent, attenuated, and avirulent Mycoplasma pneumoniae strains. J Bacteriol 100:1037-1043.

204. Tully JG, Whitcomb RF, Clark HF, Williamson DL. 1977. Pathogenic Mycoplasmas: Cultivation and Vertebrate Pathogenicity of a New Spiroplasma, p 892. Science.

205. Krause DC, Leith DK, Wilson RM, Baseman JB. Identification of Mycoplasma pneumoniae proteins associated with hemadsorption and Virulence. Identification

of Mycoplasma pneumoniae proteins associated with hemadsorption and Virulence.

206. Chen L, Leman D, Williams CR, Brooks K, Krause DC, Locklin J. 2017. A Versatile Methodology for Glycosurfaces: Direct Ligation of Nonderivatized Reducing Saccharides to Poly(pentafluorophenyl acrylate) Grafted Surfaces via Hydrazide Conjugation. Langmuir.

207. Purcell RH, Taylor-Robinson D, Wong D, Chanock RM. 1966. Color test for the measurement of antibody to T-strain mycoplasmas. Journal of bacteriology 92:6-12.

208. Baseman JB, Banai M, Kahane I. 1982. Sialic acid residues mediate Mycoplasma pneumoniae attachment to human and sheep erythrocytes. Infect Immun 38:389-91.

209. Driks A. 2011. Tapping into the biofilm: insights into assembly and disassembly of a novel amyloid fibre in Bacillus subtilis. Molecular microbiology 80:1133-1136.

210. Manchee RJ, Taylor-Robinson D. 1969. Utilization of neuraminic acid receptors by mycoplasmas. J Bacteriol 98:914-919.

211. Miyata M. 2008. Molecular Mechanism of *Mycoplasma* gliding - A Novel Cell Motility System. Springer New York.

212. Kogure T, Suzuki T, Takahashi T, Miyamoto D, Hidari KI, Guo CT, Ito T, Kawaoka Y, Suzuki Y. 2006. Human trachea primary epithelial cells express both sialyl(alpha2-3)Gal receptor for human parainfluenza virus type 1 and avian

influenza viruses, and sialyl(alpha2-6)Gal receptor for human influenza viruses. Glycoconj J 23:101-6.

213. Razin S, Kahane I, Banai M, Bredt W. 1981. Adhesion of mycoplasmas to eukaryotic cells. Ciba Found Symp 80:98-118.

214. Leith DK, Hansen EJ, Wilson RM, Krause DC, Baseman JB. 1983. Hemadsorption and virulence are separable properties of Mycoplasma pneumoniae. Infect Immun 39:844-850.

215. Krause DC, Leith DK, Baseman JB. 1983. Reacquisition of specific proteins confers virulence in Mycoplasma pneumoniae. Infect Immun 39:830-836.

216. Peng W, de Vries RP, Grant OC, Thompson AJ, McBride R, Tsogtbaatar B, Lee PS, Razi N, Wilson IA, Woods RJ, Paulson JC. 2017. Recent H3N2 Viruses Have Evolved Specificity for Extended, Branched Human-type Receptors, Conferring Potential for Increased Avidity. Cell Host Microbe 21:23-34.

217. Viswanathan K, Koh X, Chandrasekaran A, Pappas C, Raman R, Srinivasan A, Shriver Z, Tumpey TM, Sasisekharan R. 2010. Determinants of glycan receptor specificity of H2N2 influenza A virus hemagglutinin. PLoS One 5:e13768.

218. Nicholls JM, Bourne AJ, Chen H, Guan Y, Peiris JS. 2007. Sialic acid receptor detection in the human respiratory tract: evidence for widespread distribution of potential binding sites for human and avian influenza viruses. Respir Res 8:73.

219. Matrosovich MN, Matrosovich TY, Gray T, Roberts NA, Klenk HD. 2004. Human and avian influenza viruses target different cell types in cultures of human airway epithelium. Proc Natl Acad Sci U S A 101:4620-4.